DOA Estimation for Transmit Beamspace MIMO Radar via Tensor Decomposition With Vandermonde Factor Matrix

Feng Xu, *Member, IEEE*, Matthew W. Morency, *Member, IEEE*, and Sergiy A. Vorobyov, *Fellow, IEEE*

***Abstract*—We address the problem of tensor decomposition in application to direction-of-arrival (DOA) estimation for two-dimensional transmit beamspace (TB) multiple-input multiple-output (MIMO) radar. A general higher-order tensor model that enables computationally efficient DOA estimation is designed. Whereas other tensor decomposition-based methods treat all factor matrices as arbitrary, the essence of the proposed DOA estimation method is to fully exploit the Vandermonde structure of the factor matrices to take advantage of the shift-invariance between and within different transmit subarrays. Specifically, the received signal of TB MIMO radar is expressed as a higher-order tensor. A computationally efficient tensor decomposition method is proposed to decompose the Vandermonde factor matrices. The generators of the Vandermonde factor matrices are computed to estimate the phase rotations between subarrays, which can be utilized as a look-up table for finding target DOAs. The proposed tensor model and the DOA estimation algorithm are also straightforwardly applicable for the one-dimensional TB MIMO radar case. It is further shown that our proposed approach can be used in a more general scenario where the transmit subarrays with arbitrary but identical configuration can be non-uniformly displaced. We also show that both the tensor rank of the signal tensor and the matrix rank of a particular matrix derived from the signal tensor are identical to the number of targets. Thus, the number of targets can be estimated via matrix rank determination. Simulation results illustrate the performance improvement of the proposed DOA estimation method as compared to other tensor decomposition-based techniques for TB MIMO radar.**

***Index Terms*—DOA estimation, shift-invariance, TB MIMO radar, tensor decomposition, vandermonde factor matrix.**

I. Introduction

THE development of multiple-input multiple-output (MIMO) radar has been the focus of intensive research [1]–[5] over the last decade, and has opened new opportunities in target detection and parameter estimation. Many works have been reported in the literature showing the applications of MIMO radar with widely separated antennas [1] or collocated antennas [2]. Among these applications, direction-of-arrival (DOA) estimation [3], [6]–[16] is one of the most fundamental research topics. In this paper, we mainly focus on the DOA estimation problem for MIMO radar with collocated antennas.

By ensuring that the transmitted waveforms are orthogonal [17], MIMO radar enables increasing the system's degrees of freedom (DoF), improving the spatial resolution and enhancing the parameter identifiability. The essence behinds these advantages is the construction of a virtual array (VA), which can be regarded as a new array with larger aperture and more elements [4], [5]. However, the omnidirectional transmit beampattern in MIMO radar, resulting from the orthogonal waveforms, deteriorates the parameter estimation performance since most of the emitted energy is wasted as compared to its phased-array counterpart. To tackle this problem, the transmit beamspace (TB) technique has been introduced [3], [6], [18]. In TB MIMO radar, the transmitted energy can be focused on a fixed spatial region [3], [6] by using a number of linear combinations of the transmitted waveforms via a TB matrix. This benefit becomes more evident when the number of elements in MIMO radar is large [18]. Specifically, at some number of waveforms, the gain from using more waveforms begins to degrade the estimation performance. The trade-off between waveform diversity and spatial diversity implies that the performance of DOA estimation in TB MIMO radar can be further improved with a carefully designed TB matrix.

Meanwhile, many algorithms for DOA estimation in MIMO radar have been proposed. These algorithms can be classified into two categories, signal covariance matrix-based algorithms [3], [6]–[10] and signal tensor decomposition-based algorithms [11]–[16], [19]–[24]. For example, the estimation of target spatial angles can be conducted by multiple signal classification (MUSIC). The generalization of MUSIC to a planar array requires a two-dimensional (2-D) spectrum searching [7], and thus suffers from high computational complexity. By exploiting the rotational invariance property (RIP) of the signal subspace, estimation of signal parameters via rotational invariance technique (ESPRIT) [3], [6], [8] can be applied to estimate the target angles without a spectrum searching. The RIP can be enforced in many ways, e.g., uniformly spaced antennas [8]

Manuscript received December 6, 2021; revised April 7, 2022 and May 2, 2022; accepted May 10, 2022. Date of publication May 20, 2022; date of current version June 17, 2022. The associate editor coordinating the review of this manuscript and approving it for publication was Dr. Evrim Acar. This work was supported in part by the Academy of Finland under Grant 319822, in part by Huawei, and in part by China Scholarship Council. *(Corresponding author: Sergiy A. Vorobyov.)*

Feng Xu was with the School of Information and Electronics, Beijing Institute of Technology, Beijing 100081, China. He is now with Department of Signal Processing and Acoustics, Aalto University, 02150 Espoo, Finland (e-mail: feng.xu@aalto.fi).

Matthew W. Morency is with Nokia Networks in Espoo, 02150 Espoo, Finland (e-mail: matthew.morency@nokia.com).

Sergiy A. Vorobyov is with the Department of Signal Processing and Acoustics, Aalto University, 02150 Espoo, Finland (e-mail: svor@ieee.org).

This article has supplementary downloadable material available at https://doi.org/10.1109/TSP.2022.3176092, provided by the authors.

Digital Object Identifier 10.1109/TSP.2022.3176092

and the design of TB matrix [3], [6]. To further reduce the computational complexity and increase the number of snapshots, unitary-ESPRIT (U-ESPRIT) has been proposed [10]. Some algorithms, like propagator method (PM), have been studied [9] to avoid the singular value decomposition (SVD) of the signal covariance matrix. The aforementioned DOA estimation algorithms are mostly conducted on a per-pulse basis to update the result from pulse to pulse. They ignore the multi-linear structure of the received signal in MIMO radar and, therefore, lead to poor performance in low signal-to-noise ratio (SNR) region.

Algorithms that belong to the second category, signal tensor decomposition-based algorithms, have been proposed to address the problem of poor performance in low SNR. In particular, a 3-order tensor is introduced to store the whole received signal for MIMO radar in a single coherent processing interval (CPI). Methods like high-order SVD (HOSVD) [14]–[16] and canonical decomposition/ parallel factor (CANDECOMP/PARAFAC, CP) analysis [11]–[13] can be applied to decompose the factor matrices. The DOA estimation can be conducted by exploiting the factor matrix with the target angular information. For example, the widely used alternating least squares (ALS) algorithm is a common way of computing the approximate low-rank factors of a tensor. These factor matrices can be used to locate multiple targets simultaneously [11], [19]. Although the application of the conventional ALS algorithm improves the DOA estimation performance for MIMO radar, it usually requires the tensor rank in order to be initialized, and the computational complexity can be extremely high as the convergence is unstable.

Nevertheless, conventional tensor decomposition methods are developed for tensors with arbitrary factor matrices. In array signal processing, special matrix structure like Toeplitz, Hankel, Vandermonde and columnwise orthonormal [20], [25] may exist in factor matrix when a tensor model is applied to collect the received signal. The most common special structure, Vandermonde, can be generated from the application of carrier frequency offset, e.g., frequency diversity array (FDA) [26] and orthogonal frequency-division multiplexing (OFDM) waveform [27], or uniformly spaced antennas, e.g., uniform linear array (ULA) and uniform rectangular array (URA). While conventional tensor decomposition methods are usually designed for tensors with arbitrary factor matrices, the decomposition of a tensor with structured factor matrices deserves further study as the structured factor matrix may point to a novel decomposition method and better uniqueness conditions. This is called *constrained tensor decomposition* [20], [25], [28]–[30]. Moreover, transmit array interpolation is introduced for MIMO radar with arbitrary array structure [14]. By solving the minimax optimization problem for interpolation matrix design, the original transmit array is mapped to a virtual array with desired structure. The DOA estimation bias caused by interpolation errors has also been analyzed in [14]. However, the interpolation technique deteriorates the parameter identifiability, which makes it inappropriate for TB MIMO radar with arbitrary but identical subarrays wherein the additional structures can be used for improving performance.

In this paper, we consider the problem of tensor decomposition in application to DOA estimation for TB MIMO radar with multiple transmit subarrays.[1] A general higher-order tensor model that enables computationally efficient DOA estimation is designed. Whereas other tensor decomposition-based methods treat all factor matrices as arbitrary, the proposed DOA estimation method fully exploits the Vandermonde structure of the factor matrix to take advantage of the shift-invariance between and within different transmit subarrays. In particular, the received signal of TB MIMO radar is expressed as a higher-order tensor. A computationally efficient tensor decomposition method, which can be conducted via linear algebra with no iterations, is proposed to decompose the factor matrices. Then, the Vandermonde structure of the factor matrices is utilized to estimate the phase rotations between transmit subarrays, which can be applied as a look-up table for finding targets DOA. It is further shown that our proposed method can be used in a more general scenario where the subarray configurations are arbitrary but identical. By exploiting the shift-invariance, the proposed method improves the DOA estimation performance over conventional tensor decomposition-based methods for TB MIMO radar. Since both the tensor rank and the matrix rank of the designed signal model are identical to the number of targets, the number of targets can be estimated if it is unknown via matrix rank determination instead of solving the NP-hard tensor rank estimation problem. The tensor model as well as the algorithms are developed for the general case of 2-D TB MIMO radar, while they are straightforwardly applicable (with some further simplifications) for the case of one-dimensional (1-D) TB MIMO radar as well. Simulation results verify that the proposed DOA estimation method has better accuracy and higher resolution than the existing methods that can be used in the context.

The rest of this paper is organized as follows. Some multi-algebra preliminaries about tensors and matrices are introduced. A higher-order tensor model for TB MIMO radar with uniformly spaced transmit subarrays is designed in Section II. In Section III, the proposed tensor model is properly reshaped in order to tackle the problem of rank deficiency caused by identical target Doppler shifts. The DOA estimation is conducted by exploiting the shift-invariance between and within different subarrays. Parameter identifiability is analyzed while the number of targets estimation is discussed. Section IV generalizes the proposed DOA estimation approach to TB MIMO radar with non-uniformly spaced transmit subarrays. Section V performs the simulation examples while the conclusions are drawn in Section VI.

Notation: Scalars, vectors, matrices and tensors are denoted by lowercase, boldface lowercase, boldface uppercase, and calligraphic letters, e.g., y, $\mathbf{y}$, $\mathbf{Y}$, and $\mathcal{Y}$, respectively. The transposition, Hermitian transposition, inversion, pseudo-inversion, Hadamard product, outer product, Kronecker product and Khatri-Rao (KR) product operations are denoted by $(\cdot)^T$, $(\cdot)^H$, $(\cdot)^{-1}$, $(\cdot)^\dagger$, $*$, $\circ$, $\otimes$, and $\odot$, respectively, while $vec(\cdot)$ stands for the operator which stacks the elements of a matrix/tensor one by one to a column vector. The notation $diag(\mathbf{y})$

[1] Some preliminary ideas that have been extended and developed to this paper were published in [28], [31].

represents a diagonal matrix with its elements being the elements of $\mathbf{y}$, while $\|\mathbf{Y}\|_F$ and $\|\mathbf{Y}\|$ are the Frobenius norm and Euclidean norm of $\mathbf{Y}$, respectively. Moreover, $\mathbf{1}_{M\times N}$ and $\mathbf{0}_{M\times N}$ denote an all-one matrix of dimension $M \times N$ and an all-zero matrix of size $M \times N$, respectively, and $\mathbf{I}_M$ stands for the identity matrix of size $M \times M$. For a matrix $\mathbf{B} \in \mathbb{C}^{M\times N}$, the n-th column vector and (m,n)-th element are denoted by $\mathbf{b}_n$ and B_{mn}, respectively, while the m-th element of a vector $\mathbf{b} \in \mathbb{C}^M$ is given by $b(m)$. The estimates of $\mathbf{B}$ and $\mathbf{b}$ are given by $\hat{\mathbf{B}}$ and $\hat{\mathbf{b}}$, while the rank and Kruskal-rank of $\mathbf{B}$ are denoted by $r(\mathbf{B})$ and $k(\mathbf{B})$, respectively. To express two submatrices of $\mathbf{B}$, one without the first and the other without the last row vector, the notations $\underline{\mathbf{B}}$ and $\overline{\mathbf{B}}$, respectively, are applied. If $\mathbf{B}$ can be written as $\mathbf{B} \triangleq [\mathbf{b}_1, \mathbf{b}_2, \ldots, \mathbf{b}_N] \in \mathbb{C}^{M\times N}$, where $\mathbf{b}_n \triangleq [b_n, b_n^2, \ldots, b_n^M]^T \in \mathbb{C}^M$, it is a Vandermonde matrix, and $\boldsymbol{\beta} \triangleq [b_1, b_2, \ldots, b_N]^T \in \mathbb{C}^N$ is the vector of generators. When each element is unique, $\boldsymbol{\beta}$ is considered to be distinct.

The following equalities hold true:

$$\begin{aligned}
&\mathbf{A} \odot \mathbf{b}^T = \mathbf{b}^T \odot \mathbf{A} \\
&\mathbf{A} \odot \mathbf{b}^T \odot \mathbf{C} = \mathbf{b}^T \odot \mathbf{A} \odot \mathbf{C} = \mathbf{A} \odot \mathbf{C} \odot \mathbf{b}^T \\
&(\mathbf{A} \odot \mathbf{B}) \odot \mathbf{C} = \mathbf{A} \odot (\mathbf{B} \odot \mathbf{C}) \\
&vec\left(\mathbf{A}diag(\mathbf{b})\mathbf{D}\right) = \left(\mathbf{D}^T \odot \mathbf{A}\right)\mathbf{b} \\
&(\mathbf{A} \otimes \mathbf{C})(\mathbf{D} \otimes \mathbf{E}) = (\mathbf{AD}) \otimes (\mathbf{CE}),
\end{aligned} \tag{1}$$

where $\mathbf{A} \in \mathbb{C}^{M\times N}$, $\mathbf{C} \in \mathbb{C}^{Q\times N}$, $\mathbf{D} \in \mathbb{C}^{N\times P}$, $\mathbf{E} \in \mathbb{C}^{N\times L}$ and $\mathbf{B} = diag(\mathbf{b}) \in \mathbb{C}^{N\times N}$.

A. Algebra Preliminaries for Tensors

For an N-th order tensor $\mathcal{Y} \in \mathbb{C}^{I_1\times I_2\times\cdots\times I_N}$, the following facts are introduced [19], [32], [33].

Fact 1 (PARAFAC decomposition): The PARAFAC decomposition of an N-th order tensor is a linear combination of the minimum number of rank-one tensors, given by

$$\mathcal{Y} = \sum_{l=1}^{L} \mathbf{a}_l^{(1)} \circ \mathbf{a}_l^{(2)} \circ \cdots \circ \mathbf{a}_l^{(N)} \triangleq \left[\!\left[\mathbf{A}^{(1)}, \mathbf{A}^{(2)}, \ldots, \mathbf{A}^{(N)}\right]\!\right], \tag{2}$$

where $\mathbf{a}_l^{(n)}$ is the l-th column of $\mathbf{A}^{(n)}$ with $\mathbf{A}^{(n)}$ being the n-th factor matrix of size $I_n \times L$, and L is the tensor rank.

Fact 2 (Uniqueness of PARAFAC decomposition): The PARAFAC decomposition is unique if all potential factor matrices satisfying (1) also match with

$$\tilde{\mathbf{A}}^{(n)} = \mathbf{A}^{(n)}\boldsymbol{\Pi}\boldsymbol{\Delta}^{(n)}, \tag{3}$$

where $\boldsymbol{\Pi}$ is a permutation matrix and $\boldsymbol{\Delta}^{(n)}$ is a diagonal matrix. The product of $\boldsymbol{\Delta}^{(n)}, n = 1, 2, \ldots, N$ is an $L \times L$ identity matrix. Usually, the generic uniqueness condition is given by [32], [33]:

$$\sum_{n=1}^{N} k(\mathbf{A}^{(n)}) \geq 2L + (N-1). \tag{4}$$

Fact 3 (Mode-n tall matrix unfolding): The mode-n tall matrix unfolding (as known as n-th multi-mode/mixed-mode unfolding) of a tensor $\mathcal{Y} \in \mathbb{C}^{I_1\times I_2\times\cdots\times I_N}$ gives a matrix $\mathbf{Y}_{(n)}$ of size $I_1 \cdots I_{n-1} I_{n+1} \cdots I_N \times I_n$

$$\mathbf{Y}_{(n)} = \left(\mathbf{A}^{(1)} \cdots \odot \mathbf{A}^{(n-1)} \odot \mathbf{A}^{(n+1)} \cdots \odot \mathbf{A}^{(N)}\right)\left(\mathbf{A}^{(n)}\right)^T. \tag{5}$$

Fact 4 (Tensor reshape): The reshape operator for an N-th order tensor $\mathcal{Y} \in \mathbb{C}^{I_1\times I_2\times\cdots\times I_N}$ returns a new M-th order tensor $\mathcal{X} \in \mathbb{C}^{J_1\times J_2\times\cdots\times J_M}$ with $\prod_{n=1}^{N} I_n = \prod_{m=1}^{M} J_m$ and $vec(\mathcal{Y}) = vec(\mathcal{X})$.[2]

Lemma 1: Consider a 3-order tensor $\mathcal{Y} \triangleq \left[\!\left[\mathbf{A}^{(1)}, \mathbf{A}^{(2)}, \mathbf{A}^{(3)}\right]\!\right]$, where $\mathbf{A}^{(1)}$ is the KR product of two Vandermonde matrices $\mathbf{B} \in \mathbb{C}^{p\times L}$ and $\mathbf{C} \in \mathbb{C}^{q\times L}$, $pq = I_1$, and $\mathbf{A}^{(3)}$ is a tall matrix that has column full rank. Assuming that matrices $\mathbf{B}$ and $\mathbf{C}$ have distinct generators, the decomposition of $\mathcal{Y}$ is generically unique if

$$\min((p-1)q, (q-1)p) \geq \frac{L}{I_2}. \tag{6}$$

Proof: See Appendix A.

II. TB MIMO Radar Tensor Model

Consider a collocated MIMO radar with $M = M_x M_y$ transmit antenna elements and N receive antenna elements. The transmit array is a URA with its elements spaced at half the working wavelength away from each other in both directions, as shown in Fig. 1. The receive elements are randomly placed within a fixed planar array. The $M \times 1$ transmit steering vector can be given by

$$\mathbf{a}(\theta, \varphi) = \mathbf{u}(\theta, \varphi) \otimes \mathbf{v}(\theta, \varphi), \tag{7}$$

where $\mathbf{u}(\theta,\varphi) \triangleq \left[1, e^{-j\pi u}, \ldots, e^{-j(M_y-1)\pi u}\right]^T \in \mathbb{C}^{M_y}$, $\mathbf{v}(\theta,\varphi) \triangleq \left[1, e^{-j\pi v}, \ldots, e^{-j(M_x-1)\pi v}\right]^T \in \mathbb{C}^{M_x}$, $u \triangleq \sin\varphi\sin\theta$ and $v \triangleq \sin\varphi\cos\theta$ are the spatial frequencies in different directions, and (θ, φ) is the pair of azimuth and elevation of a target. The steering vector of the receive array can be written as $\mathbf{b}(\theta,\varphi) \triangleq \left[1, e^{-j\frac{2\pi}{\lambda}(x_2 v + y_2 u)}, \ldots, e^{-j\frac{2\pi}{\lambda}(x_N v + y_N u)}\right]^T \in \mathbb{C}^N$, where $\{(x_n, y_n) | 0 < x_n \leq D_x, 0 < y_n \leq D_y\}$ are the

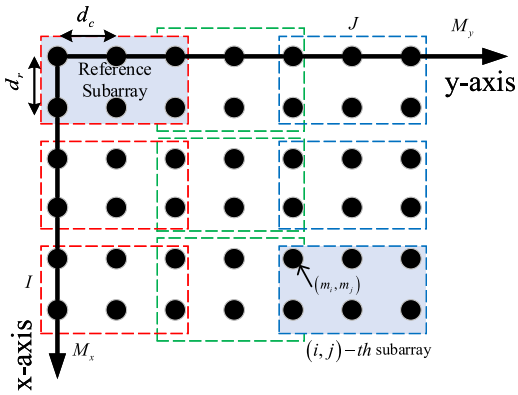

Fig. 1. Transmit array configuration for TB MIMO radar with planar array.

[2]The equity depends on the way the modes are combined in each tensor. More discussions can be found in Appendix B in the supplemental material.

coordinates of the receive elements, λ is the working wavelength, and D_x, D_y denote the receive array apertures in two directions, respectively.

Assume $S = IJ$ transmit subarrays are uniformly spaced at the transmit side, which can be overlapped or not. Each of them contains $M_0 = M_{x_0} M_{y_0}$ elements. For (i,j)-th transmit subarray (or equivalently, for s-th transmit subarray where $s = (j-1)I + i$), the index of the first element is denoted by $(m_i, m_j),\ i = 1, 2, \ldots, I,\ j = 1, 2, \ldots, J$. Both m_i and m_j rise uniformly. The first transmit subarray is selected as the reference transmit subarray. The $M_0 \times 1$ steering vector of the reference transmit subarray at direction (θ, φ) can be written as $\mathbf{a}_0(\theta,\varphi) = \mathbf{u}_0(\theta,\varphi) \otimes \mathbf{v}_0(\theta,\varphi)$, where $\mathbf{u}_0(\theta,\varphi) \in \mathbb{C}^{M_{y_0}}$ and $\mathbf{v}_0(\theta,\varphi) \in \mathbb{C}^{M_{x_0}}$ contain the first M_{y_0} and M_{x_0} elements in $\mathbf{u}(\theta,\varphi)$ and $\mathbf{v}(\theta,\varphi)$, respectively.

For L targets in $\{(\theta_l, \varphi_l)\}_{l=1}^{L}$, the transmit and receive steering matrices can be generalized as $\mathbf{A} \triangleq [\mathbf{a}(\theta_1,\varphi_1), \mathbf{a}(\theta_2,\varphi_2), \ldots, \mathbf{a}(\theta_L,\varphi_L)] \in \mathbb{C}^{M \times L}$ and $\mathbf{B} \triangleq [\mathbf{b}(\theta_1,\varphi_1), \mathbf{b}(\theta_2,\varphi_2), \ldots, \mathbf{b}(\theta_L,\varphi_L)] \in \mathbb{C}^{N \times L}$, respectively. Note that the transmit array is a URA, thus, we have

$$\mathbf{A} = \mathbf{U} \odot \mathbf{V}, \tag{8}$$

where $\mathbf{U} \triangleq [\mathbf{u}(\theta_1,\varphi_1), \mathbf{u}(\theta_2,\varphi_2), \ldots, \mathbf{u}(\theta_L,\varphi_L)] \in \mathbb{C}^{M_y \times L}$ and $\mathbf{V} \triangleq [\mathbf{v}(\theta_1,\varphi_1), \mathbf{v}(\theta_2,\varphi_2), \ldots, \mathbf{v}(\theta_L,\varphi_L)] \in \mathbb{C}^{M_x \times L}$. Similarly, the $M_0 \times L$ steering matrix for the reference transmit subarray can be denoted by

$$\mathbf{A}_0 = \mathbf{U}_0 \odot \mathbf{V}_0, \tag{9}$$

where $\mathbf{U}_0 \in \mathbb{C}^{M_{y_0} \times L}$ and $\mathbf{V}_0 \in \mathbb{C}^{M_{x_0} \times L}$ are the submatrices of $\mathbf{U}$ and $\mathbf{V}$ that consist of the first M_{y_0} and M_{x_0} rows, respectively. Then, let us consider the $M_0 \times L$ steering matrix for the (i,j)-th transmit subarray, which can be given by

$$\mathbf{A}_{ij} = \mathbf{U}_j \odot \mathbf{V}_i, \tag{10}$$

where $\mathbf{U}_j = \mathbf{U}_0 \boldsymbol{\Gamma}_j$, $\mathbf{V}_i = \mathbf{V}_0 \boldsymbol{\Delta}_i$, $\boldsymbol{\Gamma}_j = diag(\boldsymbol{\gamma}_j), \boldsymbol{\Delta}_i = diag(\boldsymbol{\delta}_i)$, vectors $\boldsymbol{\gamma}_j \triangleq \left[e^{-j\pi(m_j-1)u_1}, \ldots, e^{-j\pi(m_j-1)u_L}\right]^T \in \mathbb{C}^L$ and $\boldsymbol{\delta}_i \triangleq \left[e^{-j\pi(m_i-1)v_1}, \ldots, e^{-j\pi(m_i-1)v_L}\right]^T \in \mathbb{C}^L$ indicate the phase rotations for L targets in two directions, respectively. It can be further shown that

$$\mathbf{A}_{ij} = \mathbf{A}_0 \boldsymbol{\Delta}_i \boldsymbol{\Gamma}_j. \tag{11}$$

In conventional MIMO radar, the received signal at the output of the receive antenna array after matched-filtering in matrix form can be modelled as [11]:

$$\mathbf{Y}_{\text{conv}} = \mathbf{B}\boldsymbol{\Sigma}\mathbf{A}^T + \mathbf{N}_{\text{conv}}, \tag{12}$$

where $\boldsymbol{\Sigma} = diag(\boldsymbol{\sigma})$, $\boldsymbol{\sigma} \triangleq \left[\sigma_1^2, \sigma_2^2, \ldots, \sigma_L^2\right]^T$ represents the vector of target radar cross section (RCS) fading coefficients obeying Swerling I model, and $\mathbf{N}_{\text{conv}} \in \mathbb{C}^{N \times M}$ is the noise matrix. When the TB technique is used [3], [6], [24], the received signal model after matched-filtering of K orthogonal waveforms[3] can be generalized as

$$\mathbf{Y}_{\text{TB}} = \mathbf{B}\boldsymbol{\Sigma}\left(\mathbf{W}^H\mathbf{A}\right)^T + \mathbf{N}_{\text{TB}}, \tag{13}$$

where $\mathbf{W} \in \mathbb{C}^{M \times K}$ denotes the TB matrix and $\mathbf{N}_{\text{TB}} \in \mathbb{C}^{N \times K}$ is the noise matrix.

Hence, the received signal for the (i,j)-th transmit subarray and the whole receive array can be written as

$$\mathbf{Y}_{ij} = \mathbf{B}\boldsymbol{\Sigma}\left(\mathbf{W}_{ij}^H\mathbf{A}_{ij}\right)^T + \mathbf{N}_{ij}, \tag{14}$$

where $\mathbf{W}_{ij} \in \mathbb{C}^{M_0 \times K}$ represents the TB matrix and $\mathbf{N}_{ij} \in \mathbb{C}^{N \times K}$ is the noise component between the (i,j)-th transmit subarray and the whole receive array. Assuming that the TB matrices for all subarrays are identical and denoted by $\mathbf{W}_0 \triangleq [\mathbf{w}_1, \mathbf{w}_2, \ldots, \mathbf{w}_K] \in \mathbb{C}^{M_0 \times K}$, after substituting (11) into (14) and vectorizing it, we have

$$\mathbf{y}_{ij} = \left[\left(\mathbf{W}_0^H\mathbf{A}_0\right) \odot \mathbf{B}\right] \boldsymbol{\Delta}_i\boldsymbol{\Gamma}_j\boldsymbol{\sigma} + \mathbf{n}_{ij}, \tag{15}$$

where $\mathbf{n}_{ij} \in \mathbb{C}^{KN}$ is the vectorized noise residue.

Considering the Doppler effect [11], the received signal for the (i,j)-th transmit subarray and the whole receive array during the q-th pulse in a single CPI, $q = 1, 2, \ldots, Q$, can be written as

$$\mathbf{y}_{ij}^{(q)} = \left[\left(\mathbf{W}_0^H\mathbf{A}_0\right) \odot \mathbf{B}\right] \boldsymbol{\Delta}_i\boldsymbol{\Gamma}_j\boldsymbol{\xi}_q + \mathbf{n}_{ij}^{(q)}, \tag{16}$$

where $\boldsymbol{\xi}_q \triangleq \left[\sigma_1^2 e^{j2\pi f_1 qT}, \sigma_2^2 e^{j2\pi f_2 qT}, \ldots, \sigma_L^2 e^{j2\pi f_L qT}\right]^T \in \mathbb{C}^L$, f_l denotes the Doppler shift, T is the radar pulse duration, and $\mathbf{n}_{ij}^{(q)} \in \mathbb{C}^{KN}$ is the vectorized noise residue in the q-th pulse.

Let us concatenate the received signal of S subarrays in the q-th pulse, i.e., $\mathbf{Y}^{(q)} \triangleq \left[\mathbf{y}_{11}^{(q)}, \ldots, \mathbf{y}_{I1}^{(q)}, \mathbf{y}_{12}^{(q)}, \ldots, \mathbf{y}_{I2}^{(q)}, \ldots, \mathbf{y}_{1J}^{(q)}, \ldots, \mathbf{y}_{IJ}^{(q)}\right] \in \mathbb{C}^{KN \times S}$. To derive the compact form, we first concatenate all I vectors together to form totally J matrices of identical dimension $KN \times I$. These matrices are denoted by $\mathbf{Y}_j^{(q)}$, and are given as

$$\mathbf{Y}_j^{(q)} = \left[\left(\mathbf{W}_0^H\mathbf{A}_0\right) \odot \mathbf{B}\right] \left(\boldsymbol{\xi}_q^T \odot \boldsymbol{\gamma}_j^T \odot \mathbf{D}\right)^T + \mathbf{N}_j^{(q)}, \tag{17}$$

where $\mathbf{D} \triangleq [\boldsymbol{\delta}_1, \boldsymbol{\delta}_2, \ldots, \boldsymbol{\delta}_I]^T \in \mathbb{C}^{I \times L}$ and $\mathbf{N}_j^{(q)} \triangleq \left[\mathbf{n}_{1j}^{(q)}, \mathbf{n}_{2j}^{(q)}, \ldots, \mathbf{n}_{Ij}^{(q)}\right] \in \mathbb{C}^{KN \times I}$.[4] Using (1), we have

$$\mathbf{Y}_j^{(q)} = \left[\left(\mathbf{W}_0^H\mathbf{A}_0\right) \odot \mathbf{B}\right] \boldsymbol{\Xi}_q\left(\boldsymbol{\gamma}_j^T \odot \mathbf{D}\right)^T + \mathbf{N}_j^{(q)}, \tag{18}$$

where $\boldsymbol{\Xi}_q = diag(\boldsymbol{\xi}_q)$. Since $[(\mathbf{W}_0^H\mathbf{A}_0) \odot \mathbf{B}]\boldsymbol{\Xi}_q$ is fixed, the concatenation of these J matrices merely depends on the concatenation of $(\boldsymbol{\gamma}_j^T \odot \mathbf{D})^T$. From the definition of the KR product, the concatenation of $\boldsymbol{\gamma}_j^T \odot \mathbf{D}$ is $\mathbf{G} \odot \mathbf{D}$, where $\mathbf{G} \triangleq [\boldsymbol{\gamma}_1, \boldsymbol{\gamma}_2, \ldots, \boldsymbol{\gamma}_J]^T \in \mathbb{C}^{J \times L}$. Therefore, the concatenation of the received signal $\mathbf{y}_{ij}^{(q)}$ for all S subarrays in the q-th pulse can be expressed as

$$\mathbf{Y}^{(q)} = \left[\left(\mathbf{W}_0^H\mathbf{A}_0\right) \odot \mathbf{B}\right] \boldsymbol{\Xi}_q(\mathbf{G} \odot \mathbf{D})^T + \mathbf{N}^{(q)}, \tag{19}$$

where $\mathbf{N}^{(q)} \triangleq \left[\mathbf{N}_1^{(q)}, \mathbf{N}_2^{(q)}, \ldots, \mathbf{N}_J^{(q)}\right] \in \mathbb{C}^{KN \times S}$. Then $\mathbf{z}_q = vec\left(\mathbf{Y}^{(q)}\right)$ can be formulated as

$$\mathbf{z}_q = \left[\mathbf{G} \odot \mathbf{D} \odot \left(\mathbf{W}_0^H\mathbf{A}_0\right) \odot \mathbf{B}\right] \boldsymbol{\xi}_q + \mathbf{n}_q, \tag{20}$$

[3]For finding optimal K see [3], [6]. Usually, optimal $K \leq M$.

[4]The derivations of (16) and (17) are straightforward. The details can be found in Appendix C in the supplemental material.

where $\mathbf{n}_q \in \mathbb{C}^{KNS}$ is the vectorized noise residue of $\mathbf{N}^{(q)}$. Then, concatenating the received signal for Q pulses, i.e., $\mathbf{Z} \triangleq [\mathbf{z}_1, \mathbf{z}_2, \ldots, \mathbf{z}_Q] \in \mathbb{C}^{KNS \times Q}$, the compact form can be written as

$$\mathbf{Z} = \left[\mathbf{G} \odot \mathbf{D} \odot \left(\mathbf{W}_0^H \mathbf{A}_0\right) \odot \mathbf{B}\right] \mathbf{X}^T + \mathbf{N}, \tag{21}$$

where $\mathbf{X} \triangleq [\boldsymbol{\xi}_1, \boldsymbol{\xi}_2, \ldots, \boldsymbol{\xi}_Q]^T \in \mathbb{C}^{Q \times L}$ and $\mathbf{N} \triangleq [\mathbf{n}_1, \mathbf{n}_2, \ldots, \mathbf{n}_Q] \in \mathbb{C}^{KNS \times Q}$. Similarly, we refer to $\mathbf{X}$ as the *Doppler steering matrix* since each of its columns denote the Doppler steering vector for one target (with additional RCS information). The matrix $\mathbf{G} \odot \mathbf{D}$ can be regarded as the *transmit subarray steering matrix*.

According to Fact 3, a 5-order tensor $\mathcal{Z} \in \mathbb{C}^{J \times I \times K \times N \times Q}$ whose matricized version is $\mathbf{Z}$ in (21) can be constructed as

$$\mathcal{Z} = \sum_{l=1}^{L} \mathbf{g}_l \circ \mathbf{d}_l \circ \mathbf{c}_l \circ \mathbf{b}_l \circ \mathbf{x}_l + \mathcal{N} \triangleq [[\mathbf{G}, \mathbf{D}, \mathbf{C}, \mathbf{B}, \mathbf{X}]] + \mathcal{N}, \tag{22}$$

where $\mathbf{C} \triangleq \mathbf{W}_0^H \mathbf{A}_0 \in \mathbb{C}^{K \times L}$, $\mathbf{g}_l$, $\mathbf{d}_l$, $\mathbf{c}_l$, $\mathbf{b}_l$ and $\mathbf{x}_l$ are the l-th columns of $\mathbf{G}$, $\mathbf{D}$, $\mathbf{C}$, $\mathbf{B}$ and $\mathbf{X}$, respectively, L is the tensor rank, and $\mathcal{N}$ is the noise tensor of the same size.

Note that since all transmit subarrays are uniformly spaced, $\mathbf{G}$ and $\mathbf{D}$ are Vandermonde matrices and their vectors of generators can be, respectively, denoted by

$$\begin{aligned} \boldsymbol{\omega}_x &\triangleq \left[e^{-j\pi\Delta_x v_1}, \ldots, e^{-j\pi\Delta_x v_L}\right]^T \in \mathbb{C}^L \\ \boldsymbol{\omega}_y &\triangleq \left[e^{-j\pi\Delta_y u_1}, \ldots, e^{-j\pi\Delta_y u_L}\right]^T \in \mathbb{C}^L, \end{aligned} \tag{23}$$

where $\Delta_x = m_{i+1} - m_i$ and $\Delta_y = m_{j+1} - m_j$ are the step sizes. We assume that $\boldsymbol{\omega}_x$ and $\boldsymbol{\omega}_y$ are distinct, which means that multiple targets are spatially distinct.

Although the tensor model (22) is derived using a URA, it can be reduced to the case of ULA by letting $I = 1$ (or equivalently, $J = 1$). Then $\mathbf{D}$ (or equivalently, $\mathbf{G}$) is reduced to an all-one row vector and can be removed from (21). Assuming the ULA is placed on the x-axis, the tensor model in this case is

$$\mathcal{Z} = [[\mathbf{D}, \mathbf{C}, \mathbf{B}, \mathbf{X}]] + \mathcal{N}, \tag{24}$$

which is a 4-order tensor. Alternatively, the signal tensor model for ULA case can be derived from the array design point of view. The generation of a URA in Fig. 1 consists of two steps. First, consider a single subarray composed of M_0 elements as the reference subarray. Let I replica subarrays be placed uniformly across the x-axis, which form a larger subarray at a higher level. Second, J copies of this higher level subarray are organized uniformly across the y-axis. Note that in this specific case, I subarrays at level-1 are non-overlapped, while their J counterparts at level-2 are partly overlapped. It is clear that the transmit subarray steering matrices for subarrays at level-1 and level-2 are $\mathbf{D}$ and $\mathbf{G}$, respectively. The ULA can be regarded as a URA with only one level of subarrays. Hence, the derivation of the tensor model for the ULA case is straightforward.

In TB MIMO radar, the DOA estimation problem then boils down to solving the following fitting problem

$$\min_{\left\{(\hat{\theta}_l, \hat{\varphi}_l)\right\}_{l=1}^{L}} \left\| \mathcal{Z} - [[\hat{\mathbf{G}}, \hat{\mathbf{D}}, \hat{\mathbf{C}}, \hat{\mathbf{B}}, \hat{\mathbf{X}}]] \right\|_F^2. \tag{25}$$

III. TB MIMO Radar DOA Estimation via Tensor Decomposition With Vandermonde Factor Matrix

We have shown that the received signal for TB MIMO radar with transmit subarrays can be expressed as a higher-order tensor. As compared to conventional 3-order tensor model for TB MIMO radar, the extra dimensions are extended to express the phase rotations among transmit subarrays. The designed tensor model enables us to conduct the DOA estimation via tensor decomposition.

Generally, the ALS algorithm can be applied to decompose such a tensor. However, the convergence of the ALS algorithm heavily relies on the determination of tensor rank, which is an NP-hard problem. The number of iterations in ALS algorithm is uncertain, which may lead to high computational complexity. Note that the tensor decomposition of $\mathcal{Z}$ can be regarded as the constrained tensor decomposition, since one of the factor matrices is structured by the regular array configuration. In the literature [20], [21], [25], [34], [35], the uniqueness condition of the tensor decomposition with special-structured factor matrices, e.g., Toeplitz, Hankel, Vandermonde and column-wise orthonormal, has been investigated. The structured factor matrix may change the uniqueness condition and, therefore, point to some new tensor decomposition methods.

In this section, we mainly focus on the tensor decomposition with Vandermonde factor matrix in application to DOA estimation for TB MIMO radar with uniformly spaced transmit subarrays. A computationally efficient DOA estimation method is proposed. The parameter identifiability of the designed tensor model is analyzed, while the number of targets estimation is discussed.

A. Tensor Reshape Operator for the Designed Tensor Model

To begin with, the estimation of target azimuth and elevation angles is equivalent to the estimation of two spatial frequencies. The pair of (θ_l, φ_l) can be computed by

$$\theta_l = \arctan\left(\frac{u_l}{v_l}\right), \qquad \varphi_l = \arcsin\left(\sqrt{u_l^2 + v_l^2}\right). \tag{26}$$

For the conventional signal covariance matrix-based DOA estimation methods like MUSIC and ESPRIT, the signal covariance matrix $\mathbf{R} = Q^{-1}\mathbf{Z}\mathbf{Z}^H$ is used. For the tensor decomposition-based DOA estimation methods, we need to reshape the constructed tensor model (22) properly to utilize Lemma 1. Note that the matrices $\mathbf{G}$ and $\mathbf{D}$ together contain the information on the spatial frequency parameters u_l and v_l, while the matrix $\mathbf{C}$ contains the estimation of u_l and v_l within a single transmit subarray. Both of them can be used to conduct DOA estimation. Therefore, by using Fact 4, the designed tensor $\mathcal{T} \in \mathbb{C}^{S \times K \times NQ}$ can be reformulated as

$$\mathcal{T} \triangleq [[(\mathbf{G} \odot \mathbf{D}), \mathbf{C}, (\mathbf{B} \odot \mathbf{X})]]. \tag{27}$$

It is worth noting that the desired tensor reshape operator can be regarded as a particular unfolding of the original tensor $\mathcal{Z}$, which enables the use of the following advantages.

First, it can be found that the estimation of (u_l, v_l) using the shift-invariance property among different transmit subarrays

may have spatial ambiguity problem ($\Delta_x \geq 2$ or $\Delta_y \geq 2$). The distance of phase centers between two adjacent subarrays should be no more than half the working wavelength. The array aperture is limited, which restricts the placement of transmit antennas. By using Lemma 1 to decompose $\mathcal{T}$, the two factor matrices independently provide the estimates of (u_l, v_l). The unambiguous spatial frequency information in the factor matrix $\mathbf{C}$ can be utilized to mitigate the potential grating lobes and, therefore, enables the transmit array to obtain a larger aperture. The array design is more flexible and the spatial resolution is improved.

Second, the usage of Lemma 1 requires one of the factor matrices to be column full rank. If we reshape the tensor $\mathcal{Z}$ so that the factor matrices are $\mathbf{G} \odot \mathbf{D}$, $\mathbf{C} \odot \mathbf{B}$ and $\mathbf{X}$, respectively, the rank deficiency problem may happen. When there are two targets that share similar Doppler shifts, two column vectors in $\mathbf{X}$ are considered to be linear dependent. The rank deficiency problem limits the application of Lemma 1 for DOA estimation in TB MIMO radar. However, the tensor $\mathcal{T}$ is reshaped by squeezing $\mathbf{B}$ and $\mathbf{X}$ into one dimension. The factor matrix $\mathbf{B} \odot \mathbf{X}$, as the KR product of a Vandermonde matrix and an arbitrary matrix, in general, has rank $\min\{QN, L\}$.[5] Thus, the problem of rank deficiency is solved. Consequently, two targets with identical Doppler shifts can be resolved, while the grating lobes can be eliminated by comparing the estimation result originated from $\mathbf{G} \odot \mathbf{D}$ to the distinct target angular information obtained by $\mathbf{C}$ [24], [28].

B. Proposed Computationally Efficient DOA Estimation Method for TB MIMO Radar With Uniformly Spaced Transmit Subarrays

Consider the noise-free version of the TB MIMO signal of (22). A particular unfolding of $\mathcal{Z}$ is utilized to obtain the two advantages mentioned in the previous subsection. The matricized version of (27) is given by

$$\mathbf{T} = [(\mathbf{G} \odot \mathbf{D}) \odot \mathbf{C}] (\mathbf{B} \odot \mathbf{X})^T, \tag{28}$$

where $\mathbf{G} \odot \mathbf{D}$, $\mathbf{C}$, and $\mathbf{B} \odot \mathbf{X}$ are the three factor matrices, respectively. The receive steering matrix and Doppler steering matrix are squeezed into one dimension so that Lemma 1 holds true for tensor $\mathcal{T}$. The decomposition of $\mathcal{T}$ is unique and can be utilized to obtain the factor matrices with targets DOA information.

Denote the SVD of (28) as $\mathbf{T} = \mathbf{U}\mathbf{\Lambda}\mathbf{V}^H$, where $\mathbf{U} \in \mathbb{C}^{SK \times L}$, $\mathbf{\Lambda} \in \mathbb{C}^{L \times L}$, and $\mathbf{V} \in \mathbb{C}^{NQ \times L}$.[6] According to Lemma 1, there is a nonsingular matrix $\mathbf{E} \in \mathbb{C}^{L \times L}$ such that

$$\mathbf{U}\mathbf{E} = \mathbf{G} \odot \mathbf{D} \odot \mathbf{C}. \tag{29}$$

Considering the operator of KR product, the Vandermonde structure of both $\mathbf{G}$ and $\mathbf{D}$ is exploited via

$$\begin{aligned} \mathbf{U}_2\mathbf{E} &= \underline{\mathbf{G}} \odot \mathbf{D} \odot \mathbf{C} = \left(\overline{\mathbf{G}} \odot \mathbf{D} \odot \mathbf{C}\right) \mathbf{\Omega}_y = \mathbf{U}_1\mathbf{E}\mathbf{\Omega}_y \\ \mathbf{U}_4\mathbf{E} &= \mathbf{G} \odot \underline{\mathbf{D}} \odot \mathbf{C} = \left(\mathbf{G} \odot \overline{\mathbf{D}} \odot \mathbf{C}\right) \mathbf{\Omega}_x = \mathbf{U}_3\mathbf{E}\mathbf{\Omega}_x, \end{aligned} \tag{30}$$

where $\underline{\mathbf{G}} = \overline{\mathbf{G}}\mathbf{\Omega}_y$, $\underline{\mathbf{D}} = \overline{\mathbf{D}}\mathbf{\Omega}_x$, $\mathbf{\Omega}_y = diag(\boldsymbol{\omega}_y)$, $\mathbf{\Omega}_x = diag(\boldsymbol{\omega}_x)$, $\mathbf{U}_1$, $\mathbf{U}_2$, $\mathbf{U}_3$ and $\mathbf{U}_4$ are the submatrices truncated from rows of $\mathbf{U}$, i.e.,

$$\begin{aligned} \mathbf{U}_1 &= \left[\mathbf{I}_{IK(J-1)}, \mathbf{0}_{IK(J-1)\times IK}\right] \mathbf{U} \\ \mathbf{U}_2 &= \left[\mathbf{0}_{IK(J-1)\times IK}, \mathbf{I}_{IK(J-1)}\right] \mathbf{U} \\ \mathbf{U}_3 &= \left(\mathbf{I}_J \otimes \left[\mathbf{I}_{K(I-1)}, \mathbf{0}_{K(I-1)\times K}\right]\right) \mathbf{U} \\ \mathbf{U}_4 &= \left(\mathbf{I}_J \otimes \left[\mathbf{0}_{K(I-1)\times K}, \mathbf{I}_{K(I-1)}\right]\right) \mathbf{U}. \end{aligned} \tag{31}$$

Noting that $\mathbf{E}$ and $\mathbf{\Omega}_x$ are both full rank, we have $\mathbf{U}_1^\dagger\mathbf{U}_2 = \mathbf{E}\mathbf{\Omega}_x\mathbf{E}^{-1}$. Since $\mathbf{\Omega}_x$ is a diagonal matrix, the vector of generators $\boldsymbol{\omega}_x$ can be estimated as the collection of eigenvalues of the matrix $\mathbf{U}_1^\dagger\mathbf{U}_2$ via eigenvalue decomposition (EVD), and $\mathbf{E}$ is the matrix of the corresponding eigenvectors. Similarly, the generator vector $\boldsymbol{\omega}_y$ can be estimated from the EVD of the matrix $\mathbf{U}_3^\dagger\mathbf{U}_4$. Note that the pair of eigenvalues in $\boldsymbol{\omega}_x$ and $\boldsymbol{\omega}_y$ can be conducted via the matrix $\mathbf{E}$. Then, the pair of spatial frequencies (u_l, v_l) can also be recovered. Let us first assume that there is no spatial ambiguity, i.e., $\Delta_x = 1$ and $\Delta_y = 1$. Given that

$$\hat{\omega}_y(l) = e^{-j\pi\Delta_y\hat{u}_l}, \quad \hat{\omega}_x(l) = e^{-j\pi\Delta_x\hat{v}_l}, \tag{32}$$

the pair of spatial frequencies (u_l, v_l) can be computed by $\hat{u}_l = [j \ln \hat{\omega}_y(l)]/\pi$ and $\hat{v}_l = [j \ln \hat{\omega}_x(l)]/\pi$. Then, the target elevation and azimuth angles can be estimated using (26).

If $\Delta_x \geq 2$ or $\Delta_y \geq 2$, the existence of grating lobes means that there is no one-to-one relationship between the spatial frequency u_l (or equivalently, v_l) and the eigenvalue $\omega_y(l)$ (or equivalently, $\omega_x(l)$). Thus, there is an ambiguity about the targets DOA. To eliminate the grating lobes, the unambiguous targets DOA in the second factor matrix $\mathbf{C}$ can be utilized [28]. Specifically, the l-th column of the Vandermonde matrices $\mathbf{G}$ and $\mathbf{D}$ can be restored using eigenvalues $\omega_x(l)$ and $\omega_y(l)$. This process is unique with or without the existence of grating lobes. Denoting the l-th column of the first factor matrix as $\boldsymbol{\kappa}_l = \mathbf{g}_l \odot \mathbf{d}_l$, we have $\boldsymbol{\kappa}_l^H\boldsymbol{\kappa}_l = S$. Then, the following relationship holds

$$\left(\frac{\boldsymbol{\kappa}_l^H}{\boldsymbol{\kappa}_l^H\boldsymbol{\kappa}_l} \otimes \mathbf{I}_K\right) (\boldsymbol{\kappa}_l \otimes \mathbf{c}_l) = \mathbf{c}_l. \tag{33}$$

Note that $\boldsymbol{\kappa}_l \otimes \mathbf{c}_l = \mathbf{g}_l \odot \mathbf{d}_l \odot \mathbf{c}_l$, which is the l-th column of the matrix $\mathbf{G} \odot \mathbf{D} \odot \mathbf{C}$. From (29), we have $\mathbf{g}_l \odot \mathbf{d}_l \odot \mathbf{c}_l = \mathbf{U}\mathbf{e}_l$, where $\mathbf{e}_l$ is the l-th column of the nonsingular matrix $\mathbf{E}$. Hence, $\boldsymbol{\kappa}_l \otimes \mathbf{c}_l = \mathbf{U}\mathbf{e}_l$. Substituting it into (33), the l-th column of the second factor matrix $\mathbf{C}$ can be computed by

$$\mathbf{c}_l = \frac{1}{S}\left[(\mathbf{g}_l \odot \mathbf{d}_l)^H \otimes \mathbf{I}_K\right] \mathbf{U}\mathbf{e}_l. \tag{34}$$

Meanwhile, since the TB matrix $\mathbf{W}_0$ is given as a prior information, $\mathbf{c}_l = \mathbf{W}_0^H\mathbf{a}_0(\theta_l, \varphi_l)$ can be rewritten in the form of K different linear equations

$$c_l(k) = \mathbf{w}_k^H\mathbf{a}_0(\theta_l, \varphi_l), \quad k = 1, 2, \ldots, K, \tag{35}$$

[5] Although there exists no deterministic formula for the rank of the KR product of a Vandermonde matrix and an arbitrary matrix, it is generally full rank. See [20], [21], [36], [37].

[6] Here we assume that the number of targets L is given. If L is unknown, the number of dominant singular values can be regarded as the estimation of the number of targets. A method based on information theoretic criteria is introduced in Section III-D to tackle this problem.

or equivalently,

$$\mathbf{p}_k^H \mathbf{a}_0(\theta_l, \varphi_l) = 0, \quad k = 1, 2, \ldots, K, \tag{36}$$

where $\mathbf{p}_k \triangleq \mathbf{w}_k - [c_l(k), \mathbf{0}_{1\times(M-1)}]$. It can be seen that the linear equations in (36) are all satisfied as equality if and only if $||\mathbf{P}^H \mathbf{a}_0(\hat{\theta}_l, \hat{\phi}_l)||^2 = 0$, where $\mathbf{P} \triangleq [\mathbf{p}_1, \mathbf{p}_2, \ldots, \mathbf{p}_K] \in \mathbb{C}^{M_0\times K}$. Therefore, the estimation of a pair (θ_l, φ_l) can be found by solving the following convex optimization problem [28]

$$\min_{(\hat{\theta}_l, \hat{\phi}_l)} \left|\left|\mathbf{P}^H \mathbf{a}_0\left(\hat{\theta}_l, \hat{\varphi}_l\right)\right|\right|^2. \tag{37}$$

Note that the cost function can be rewritten as $\mathbf{a}_0^H(\hat{\theta}_l, \hat{\varphi}_l)\mathbf{P}\mathbf{P}^H\mathbf{a}_0(\hat{\theta}_l, \hat{\varphi}_l)$, which represents the transmit power distribution at direction $(\hat{\theta}_l, \hat{\varphi}_l)$. The minimization thus leads to the lowest transmit power, which is a deep null in the transmit beampattern generated by $\mathbf{P}$. This implies that there exists an interesting relationship between the TB MIMO radar transmit beampattern and the generalized sidelobe canceller (GSC). Since the computation is conducted column by column, the independent estimates of targets DOA from the first factor matrix and the second factor matrix are paired automatically. By comparing the estimation results to each other, the grating lobes can be mitigated. The limitation on the distance between phase centers of two adjacent subarrays is therefore eliminated.

The aforementioned DOA estimation procedure is also applicable, with some further simplifications, to TB MIMO radar in the 1-D case. In this case, consider that the ULA transmit array is placed on the x-axis and we have $J = 1$. Then $\mathbf{G}$ can be removed from the tensor model $\mathcal{Z}$. In this circumstance, only two submatrices of the left singular matrix, e.g., $\mathbf{U}_3$ and $\mathbf{U}_4$ will remain, which can be obtained from (31). The spatial frequencies can be then estimated as the eigenvalues of the matrix $\mathbf{U}_3^\dagger\mathbf{U}_4$, and the targets DOA can be recovered from the spatial frequencies in the same way as before for the 2-D case. Particularly, the minimization of (37) can be regarded as a polynomial rooting problem after rewriting the transmit subarray steering vector into a linear form [24], which can be solved efficiently. The DOA estimates obtained by (32) and (37) are independent, and the unambiguous DOA estimates can be obtained via (37) even if grating lobes exist in the case of using (32).

The primary steps for the DOA estimation in TB MIMO radar with uniformly spaced transmit subarrays are then summarized as Algorithm 1.

Algorithm 1: DOA Estimation for TB MIMO radar with Uniformly Spaced Transmit Subarrays.

Input: Observation of $\mathcal{Z} \in \mathbb{C}^{J\times I\times K\times N\times Q}$ in (22) and the number of targets L
Output: $\{\theta_l\}_{l=1}^L$ and $\{\varphi_l\}_{l=1}^L$
1 Reshape $\mathcal{Z}$ into $\mathcal{T} \in \mathbb{C}^{S\times K\times NQ}$;
2 Obtain (28) via unfolding of $\mathcal{T}$;
3 Compute the left singular matrix $\mathbf{U}$ via SVD (L can be estimated via (41) if it is not given);
4 Part I: $\mathbf{U}_1, \mathbf{U}_2, \mathbf{U}_3, \mathbf{U}_4 \leftarrow$ (31);
5 Do EVD for $\mathbf{U}_1^\dagger\mathbf{U}_2$ and $\mathbf{U}_3^\dagger\mathbf{U}_4$;
6 Store the eigenvalues as $\boldsymbol{\omega}_y$ and $\boldsymbol{\omega}_x$, respectively;
7 Collect the eigenvectors as $\mathbf{E}$;
8 Part II: **while** $l = 1, 2, \cdots, L$ **do**
9 Restore the spatial frequencies (u_l, v_l) from $\omega_y(l)$ and $\omega_x(l)$ via (32);
10 Estimate (θ_l, φ_l), where grating lobes may exist;
11 Construct $\mathbf{g}_l$ and $\mathbf{d}_l$;
12 $\mathbf{c}_l \leftarrow$ (34);
13 $\mathbf{p}_k \leftarrow \mathbf{w}_k - [c_l(k), \mathbf{0}_{1\times(M-1)}]$;
14 $\mathbf{P} \leftarrow [\mathbf{p}_1, \mathbf{p}_2, \cdots, \mathbf{p}_K]$;
15 Solve (37) and obtain the unambiguous estimates of target elevation and azimuth angles;
16 Compare them with the previous estimates (see line 10) to mitigate the potential grating lobes;
17 Store (θ_l, φ_l);
18 **end**

C. Parameter Identifiability and Computational Complexity

As mentioned in Fact 2, the generic uniqueness condition for tensor decomposition for a higher-order tensor is determined by the sum of the Kruskal ranks of the factor matrices. However, if all or some factor matrices have some special properties, the uniqueness condition can be changed. In [34], [35] (see also the reference therein), a more relaxed uniqueness condition has been proved for the tensor decomposition with one column full rank factor matrix. The well-known Kruskal condition is extended in [36] for the tensor with a Vandermonde factor matrix. The case of tensor decomposition with a Vandermonde factor matrix and a column full rank factor matrix has been investigated in [20], [38].

Note that the reshaped version $\mathcal{T}$ of the designed tensor model (22) has one column full rank factor matrix[7] and one factor matrix that is the KR product of two Vandermonde matrices (for URA case) or a Vandermonde matrix (for ULA case). If we ignore this special structure and consider only the assumption that the third factor matrix is column full rank, the uniqueness condition of tensor decomposition is given by [34], [35]

$$S(S-1)K(K-1) \geq 2L(L-1) \quad \text{and} \quad NQ \geq L. \tag{38}$$

For the ULA case, the uniqueness condition of tensor decomposition when the Vandermonde structure is additionally utilized is the same as that in [20], i.e.,

$$\min\{(S-1)K, NQ\} \geq L. \tag{39}$$

If the transmit array is a URA, the uniqueness condition is slightly different. The upper bound of the tensor rank requires that (see also Appendix A)

$$\min\{(I-1)JK, (J-1)IK, NQ\} \geq L. \tag{40}$$

Given that Q is large enough, the maximum number of targets that can be resolved is in general determined by the number of transmit subarrays and the number of orthogonal waveforms. Thus, it is worth considering increasing the number of transmit

[7]The rank of $\mathbf{B} \odot \mathbf{X}$ is $\min\{QN, L\}$ and the number of pulses Q during a single CPI is generally very large in MIMO radar.

TABLE I
THE MAXIMUM NUMBER OF TARGETS THAT CAN BE RESOLVED BY THE TENSOR $\mathcal{T}$ FOR DIFFERENT UNIQUENESS CONDITIONS WHERE $I^2 = J^2 = S = K$ AND Q IS LARGE ENOUGH

$I = J$	$S = K$	Fact 2	(38)	(39)	(40)
2	4	6	9	12	8
3	9	16	51	72	54
4	16	30	170	240	192
5	25	48	424	600	500

subarrays or transmit waveforms to improve parameter identifiability.

Table I discusses the upper bound of the tensor rank for the Kruskal condition and (38)–(40). It can be seen that (39) and (40) yield the best uniqueness conditions. For the URA case, this uniqueness condition is degraded due to the increase of the number of parameters. See [39] for more discussions about the partial identifiability of the tensor decomposition, where specific conditions for coherent sources are investigated.

Theorem 1: Under the conditions that the targets are spatially distinct and the distance between two adjacent antenna elements within a single transmit subarray is less than $\lambda/2$, the signal models (24) for 1-D case and (22) for 2-D case hold true. Moreover, if the uniqueness condition (40) is satisfied and $Q > SK/N$, Algorithm 1 is guaranteed to recover the targets' true spatial directions in the noiseless case.

Proof: See Appendix D in the supplemental material.

Computational Complexity: The most expensive steps of Algorithm 1 are the SVD of $\mathbf{T}$, the EVD of $\mathbf{U}_1^{\dagger}\mathbf{U}_2$ and $\mathbf{U}_3^{\dagger}\mathbf{U}_4$, and the estimation of (θ_l, φ_l) via $\mathbf{P}$. Under the conditions of Theorem 1, the SVD of $\mathbf{T}$ has the highest complexity. Thus, the complexity of Algorithm 1 is $\mathcal{O}(S^2K^2NQ)$, while the complexity of the ALS algorithm in one iteration is $\mathcal{O}(SKNQL)$. If (40) holds, i.e., L is comparable to SK, the computational complexity of Algorithm 1 is comparable to that of one iteration of the ALS algorithm. See Appendix E in the supplemental material for more details.

D. Number of Targets Estimation

Although the signal tensor rank estimation problem is NP-hard in general, which makes it difficult to estimate L directly, under the assumptions that have been introduced in Theorem 1, this problem can be reduced to estimating the matrix rank of $\mathbf{T}$ in (28). This is because both the tensor rank of $\mathcal{T}$ and the matrix rank of $\mathbf{T}$ are identical to L. In other word, we have identified a subclass of tensor rank estimation problems which can be solved in polynomial time.

Use SVD of $\mathbf{T}$ and denote the singular values as $\lambda_1 \geq \lambda_2 \geq \cdots \geq \lambda_{SK}$. Then the following information theoretic criteria can be utilized to estimate L [40]

$$E(l) = Q \ln \left[\frac{\left(\frac{1}{SK-l} \sum_{i=l+1}^{SK} \lambda_i \right)^{SK-l}}{\prod_{i=l+1}^{SK} \lambda_i} \right] + P(l), \qquad (41)$$

where $l = 1, 2, \ldots, SK-1$ and $P(l) = 0.5[l(2SK - l)] \ln \ln Q$. The optimal L is given by $L = \arg\min E(l)$, i.e., the L largest singular values and the corresponding singular vectors should be selected. Consequently, the knowledge of the tensor rank is not needed as a prior to initialize Algorithm 1 in contradistinction to the ALS-based DOA estimation method. The required modification is only that L is first estimated as described above.

IV. TB MIMO RADAR DOA ESTIMATION VIA TENSOR DECOMPOSITION WITH GENERALIZED VANDERMONDE FACTOR MATRIX

In previous section, we have assumed that the transmit subarrays are uniformly spaced to obtain a Vandermonde structure in the factor matrix of the designed tensor. However, such constraint on subarray structure can be relaxed. The placement of all subarrays needs not be uniform, while the configuration within a single subarray can be arbitrary. The tensor model in (22) is applicable for TB MIMO radar with any arbitrary but identical transmit subarrays, since the extended factor matrix that represents the phase rotations among transmit subarrays is merely determined by the coordinates of the transmit subarray phase centers. The difference is that the array configuration varies the structure of the factor matrix, which may cause extra steps to recover the targets DOA. A typical example has been given earlier where the unambiguous spatial frequencies in $\mathbf{C}$ are exploited to eliminate the cyclic ambiguity of spatial frequencies in $\mathbf{G} \odot \mathbf{D}$.

In the following, we discuss a more general case when the transmit subarrays are non-uniformly spaced and propose a new approach for TB MIMO radar DOA estimation via tensor decomposition with generalized Vandermonde factor matrix.

A. Tensor Model for TB MIMO Radar With Non-Uniformly Spaced Transmit Subarrays

Note that the signal modelling with respect to the spatial frequencies u and v is equivalent, that is, we can fix one of them and focus on the other one to demonstrate the design of tensor model for TB MIMO radar with non-uniformly spaced transmit subarrays. Moreover, it can be further assumed that the reference subarray is a linear array, i.e., we mainly study the problem of 1-D DOA estimation in this case.

As mentioned previously, the tensor model for 1-D TB MIMO radar with uniformly spaced transmit subarrays can be written as in (24) with $\mathbf{D} \triangleq [\boldsymbol{\delta}_1, \boldsymbol{\delta}_2, \ldots, \boldsymbol{\delta}_S]^T \in \mathbb{C}^{S \times L}$ and $\boldsymbol{\delta}_s \triangleq \left[e^{-j\pi(m_s-1)\sin\theta_1}, \ldots, e^{-j\pi(m_s-1)\sin\theta_L}\right]^T \in \mathbb{C}^L$. Here m_s is the index of the first element in the s-th transmit subarray, θ denotes the target direction in linear array, and we assume as before that there are S transmit subarrays, i.e., $s = 1, 2, \ldots, S$. The steering matrix for the reference subarray in $\mathbf{C} = \mathbf{W}_0^H \mathbf{A}_0 \in \mathbb{C}^{K \times L}$ is replaced by $\mathbf{A}_0 \triangleq [\mathbf{a}_0(\theta_1), \mathbf{a}_0(\theta_2), \ldots, \mathbf{a}_0(\theta_L)] \in \mathbb{C}^{M_0 \times L}$, where $\mathbf{a}_0(\theta) \triangleq \left[1, e^{-j\pi\sin\theta}, \ldots, e^{-j(M_0-1)\pi\sin\theta}\right]^T \in \mathbb{C}^{M_0}$ and M_0 is the number of elements in a single transmit

subarray. The other factor matrices can be expressed analogously to their counterparts in (22).

Since the transmit array geometry varies only the structure of $\mathbf{D}$ and $\mathbf{C}$, (24) is a general tensor model that can be used to collect the received signal of TB MIMO radar whose transmit array is a linear array with its elements placed on a lattice. All lattice cells are enumerated sequentially. The indices of the elements form a counted set of increasing positive integers. It can be verified that m_s must be a subset of this set, since the first element of each subarray corresponds to a unique lattice cell. Hence, m_s may increase uniformly or non-uniformly.

When m_s increases uniformly, the transmit subarrays are uniformly spaced and $\mathbf{D}$ is a Vandermonde matrix. Determined by the step size of m_s, i.e., $\Delta_s = m_{s+1} - m_s$, the configuration of adjacent transmit subarrays can be partly overlapped ($\Delta_s < M_0$) or non-overlapped ($\Delta_s \geq M_0$). The DOA estimation can be conducted in both scenarios by using Algorithm 1.

When m_s increases non-uniformly, $\mathbf{D}$ is a generalized Vandermonde matrix [41]. The computationally efficient tensor decomposition method described in Algorithm 1 cannot be used directly. We can update the tensor model (24) via matrix reconstruction.

Consider as an example $S = 7$ transmit subarrays with $m_s \in \{1, 2, 3, 5, 6, 7, 9\}$. Each subarray contains three elements, therefore, the original transmit array is a ULA with $M = 11$ elements. In this case, $\mathbf{D} \triangleq [\mathbf{d}_1, \ldots, \mathbf{d}_L] \in \mathbb{C}^{7\times L}$, where $\mathbf{d}_l \triangleq \left[1, d_l, d_l^2, d_l^4, d_l^5, d_l^6, d_l^8\right]^T \in \mathbb{C}^7$ and $d_l \triangleq e^{-j\pi \sin\theta_l}$. Substituting this into (24), the tensor model for TB MIMO radar with non-uniformly spaced transmit subarray is constructed.

Next, a matrix reconstruction approach is proposed to update this constructed tensor model.

From the structure of the set of m_s, it can be shown that $\mathbf{D}$ can be interpreted as the combination of a set of submatrices $\mathbf{D}^{(\mathrm{sub})} \in \mathbb{C}^{11\times L}$ denoting different sub-ULAs associated with various shift-invariances, i.e.,

$$\begin{aligned}
\mathbf{D}^{(\mathrm{sub})} &\triangleq \left[\left(\mathbf{D}^{(1,1)}\right)^T, \left(\mathbf{D}^{(2,1)}\right)^T, \left(\mathbf{D}^{(1,2)}\right)^T\right]^T \\
\mathbf{D}^{(1,1)} &\triangleq \left[\mathbf{d}_1^{(1,1)}, \ldots, \mathbf{d}_L^{(1,1)}\right] \in \mathbb{C}^{3\times L} \\
\mathbf{D}^{(2,1)} &\triangleq \left[\mathbf{d}_1^{(2,1)}, \ldots, \mathbf{d}_L^{(2,1)}\right] \in \mathbb{C}^{3\times L} \\
\mathbf{D}^{(1,2)} &\triangleq \left[\mathbf{d}_1^{(1,2)}, \ldots, \mathbf{d}_L^{(1,2)}\right] \in \mathbb{C}^{5\times L},
\end{aligned} \tag{42}$$

where $\mathbf{d}_l^{(1,1)} \in \mathbb{C}^3$ is selected from $\mathbf{d}_l$ with $m_s \in \{1, 2, 3\}$, $\mathbf{d}_l^{(2,1)} \in \mathbb{C}^3$ is selected from $\mathbf{d}_l$ with $m_s \in \{5, 6, 7\}$, and $\mathbf{d}_l^{(1,2)} \in \mathbb{C}^5$ is selected from $\mathbf{d}_l$ with $m_s \in \{1, 3, 5, 7, 9\}$. In other words, $\mathbf{D}^{(1,1)}$ is a submatrix of $\mathbf{D}$ that consists of the first three rows with shift-invariance $\Delta_s = 1$. The other two submatrices are formed analogously. Consequently, a generalized Vandermonde matrix can be rewritten as several Vandermonde matrices by matrix reconstruction. Note that (42) is not the only matrix reconstruction method, but it contains all transmit subarrays with a minimal distinct shift-invariance set $\{\Delta_s | \Delta_s = 1, 2\}$. The matrix reconstruction is in fact identical to the transmit subarrays selection and combination, which exploits the idea of multiple invariance ESPRIT [42].

Substituting (42) into (24), the tensor model for 1-D TB MIMO radar with non-uniformly spaced transmit subarrays is given by

$$\mathcal{Z}^{(\mathrm{sub})} = \left[\left[\mathbf{D}^{(\mathrm{sub})}, \mathbf{C}, \mathbf{B}, \mathbf{X}\right]\right] + \mathcal{N}^{(\mathrm{sub})}, \tag{43}$$

where $\mathcal{N}^{(\mathrm{sub})} \in \mathbb{C}^{11\times K\times N\times Q}$ is the corresponding noise tensor.

B. Proposed DOA Estimation Approach for TB MIMO Radar With Non-Uniformly Spaced Transmit Subarrays

We can use (43) to conduct DOA estimation via Algorithm 1. Like in (28), the matrix unfolding of the updated tensor model (43) can be written as

$$\mathbf{T}^{(\mathrm{sub})} = \left(\mathbf{D}^{(\mathrm{sub})} \odot \mathbf{C}\right)(\mathbf{B} \odot \mathbf{X})^T. \tag{44}$$

Its SVD is given by $\mathbf{T}^{(\mathrm{sub})} = \mathbf{U}^{(\mathrm{sub})}\mathbf{\Lambda}^{(\mathrm{sub})}\left(\mathbf{V}^{(\mathrm{sub})}\right)^H$. Note that the generators of the Vandermonde submatrices in $\mathbf{D}^{(\mathrm{sub})}$ provide the targets DOA information at different exponential levels, i.e., $d_l^{\Delta_s}$. To exploit the Vandermonde structure in each submatrix of $\mathbf{D}^{(\mathrm{sub})}$, an extra row selection must be applied. Taking $\mathbf{D}^{(1,1)}$, for example, and using the fact that Lemma 1 holds for (43), we can generalize (29) to obtain

$$\mathbf{D}^{(1,1)} \odot \mathbf{C} = \mathbf{U}^{(1,1)}\mathbf{E}, \tag{45}$$

where $\mathbf{U}^{(1,1)} \in \mathbb{C}^{3K\times L}$ is truncated from $\mathbf{U}^{(\mathrm{sub})}$ by a proper row selection. Knowing that $\mathbf{D}^{(1,1)}$ is a Vandermonde matrix, the submatrix $\mathbf{U}^{(1,1)}$ is further divided into two submatrices to exploit the shift-invariance $d_l^{\Delta_s}$. The further steps are then similar to that of (30)–(32), and they have been summarized previously. Thus, each column of $\mathbf{D}^{(1,1)}$ can be estimated. The estimates of $\mathbf{D}^{(1,2)}$ and $\mathbf{D}^{(2,1)}$ can be obtained analogously.

However, note that if $\Delta_s > 1$, the problem of grating lobes may still occur when recovering θ_l from $\mathbf{U}^{(N_{\Delta_s},\Delta_s)}$, where N_{Δ_s} represents the number of subarrays whose shift-invariance is determined by Δ_s. The use of Algorithm 1 for grating lobes mitigation requires each subarray to be a dense ULA, which restricts the aperture of the transmit subarray, and therefore, the spatial resolution. Meanwhile, the array manifolds of all transmit subarrays can be different if some antenna elements are disabled. The robustness of Algorithm 1 is poor under this circumstance. To tackle these problems, it is necessary to develop a new approach that can independently estimate the unambiguous targets DOA from $\mathbf{D}^{(\mathrm{sub})}$.

For every possible shift-invariance Δ_s, denote

$$\begin{aligned}
\mathbf{m}_l^{(\Delta_s)} &\triangleq \left[\overline{\mathbf{d}}_l^{(1,\Delta_s)T}, \ldots, \overline{\mathbf{d}}_l^{(N_{\Delta_s},\Delta_s)T}\right]^T \\
\mathbf{n}_l^{(\Delta_s)} &\triangleq \left[\underline{\mathbf{d}}_l^{(1,\Delta_s)T}, \ldots, \underline{\mathbf{d}}_l^{(N_{\Delta_s},\Delta_s)T}\right]^T.
\end{aligned} \tag{46}$$

To illustrate (46), consider again the array structure used in (42). The shift-invariance set contains $\Delta_s = 1, 2$. When $\Delta_s = 1$, there are two different submatrices, or in other words, sub-ULAs corresponding to the submatrices $\mathbf{D}^{(1,1)}$ and $\mathbf{D}^{(2,1)}$, respectively. Thus, we have $N_1 = 2$,

Algorithm 2: DOA Estimation for TB MIMO radar with Non-uniformly Spaced Transmit Subarrays.

Input: $\mathcal{Z} \in \mathbb{C}^{S\times K\times N\times Q}$ in (24) and L
Output: $\{\theta_l\}_{l=1}^{L}$
Matrix reconstruction $\leftarrow$ (42);
Substitute (42) into (24);
Collect the left singular matrix $\mathbf{U}^{(\mathrm{sub})} \leftarrow$ (44);
for each pair of (N_{Δ_s}, Δ_s) **do**
  Select the corresponding submatrix of $\mathbf{U}^{(\mathrm{sub})}$;
  Follow the procedures in Part I of **Algorithm 1**;
  Restore the eigenvalues that can be used to build $\mathbf{D}^{(N_{\Delta_s},\Delta_s)}$;
end
while $l = 1, 2, \cdots, L$ **do**
  $\mathbf{m}_l^{(\Delta_s)}$ and $\mathbf{n}_l^{(\Delta_s)} \leftarrow$ (46);
  $f(d_l) \leftarrow$ (48);
  Root the polynomial function $f(d_l)$;
  Select the root that nearest to the unit circle as $\hat{d}_l$;
  $\hat{\theta}_l = \arcsin\left(\frac{j\ln(\hat{d}_l)}{\pi}\right)$;
end

$\mathbf{m}_l^{(1)} = \left[\overline{\mathbf{d}}_l^{(1,1)T}, \overline{\mathbf{d}}_l^{(2,1)T}\right]^T = \left[1, d_l, d_l^4, d_l^5\right]^T$, and $\mathbf{n}_l^{(1)} = \left[\underline{\mathbf{d}}_l^{(1,1)T}, \underline{\mathbf{d}}_l^{(2,1)T}\right]^T = \left[d_l, d_l^2, d_l^5, d_l^6\right]^T$. When $\Delta_s = 2$, only one submatrix, or equivalently, sub-ULA corresponding to $\mathbf{D}^{(1,2)}$ exists, i.e., $N_2 = 1$, $\mathbf{m}_l^{(2)} = \overline{\mathbf{d}}_l^{(1,2)} = \left[1, d_l^2, d_l^4, d_l^6\right]^T$ and $\mathbf{n}_l^{(2)} = \underline{\mathbf{d}}_l^{(1,2)} = \left[d_l^2, d_l^4, d_l^6, d_l^8\right]^T$. Consequently, the following constraint should be satisfied

$$\mathbf{m}_l^{(\Delta_s)} d_l^{\Delta_s} = \mathbf{n}_l^{(\Delta_s)}. \tag{47}$$

The optimal solution d_l is unique as long as two coprime numbers can be found in the shift-invariance set $\{\Delta_s\}$ [41], which means that the grating lobes can be eliminated. The optimization of (47) can be conducted by rooting the polynomial function

$$f(d_l) \triangleq \sum_{\Delta_s\in\{\Delta_s\}} \left|\left|\mathbf{m}_l^{(\Delta_s)} d_l^{\Delta_s} - \mathbf{n}_l^{(\Delta_s)}\right|\right|_F^2. \tag{48}$$

By definition of d_l, the root nearest to the unit circle should be chosen as $\hat{d}_l$, which finally estimates the targets DOA as $\hat{\theta}_l = \arcsin(j\ln(\hat{d}_l)/\pi)$. The tenor model $\mathcal{Z}^{(\mathrm{sub})}$ enables us to conduct the unambiguous DOA estimation in a more general scenario for TB MIMO radar. The transmit subarrays can be organized in a non-uniform way. If the shift-invariance set $\{\Delta_s\}$ contains a pair of coprime integers, the problem of spatial ambiguity can be solved with no limitation on the transmit subarray structure. Hence, the structures of the transmit subarrays can be arbitrary but identical.

An outline of the proposed DOA estimation approach for TB MIMO radar with non-uniformly spaced transmit subarrays is summarized in Algorithm 2.

Remarks: For TB MIMO radar with uniformly spaced transmit subarrays, a simple way to build $\mathbf{D}^{(\mathrm{sub})}$ is to concatenate three submatrices of $\mathbf{D}$, which, respectively, consist of the odd rows, even rows and all rows. Hence, Algorithm 2 can be regarded as the generalization of Algorithm 1, which is applicable for TB MIMO radar with any arbitrary but identical transmit subarrays. It can be found that Algorithm 2 does not require the transmit subarrays to be dense ULA, the transmit array can be placed on a larger lattice to obtain a higher spatial resolution. The robustness of Algorithm 2 is better in the sense that if some elements in a transmit subarray are broken, a useful solution is to disable the elements in other subarrays accordingly to keep the manifolds identical. Moreover, we can select subsets of the elements in all subarrays to fulfill other purposes like communication in joint radar-communication system for example [43]. The extension of these remarks to the case of planar array is straightforward.

V. Simulation Results

In this section, we investigate the DOA estimation performance of the proposed method in terms of the root mean square error (RMSE) and probability of resolution of closely spaced targets for TB MIMO radar with transmit subarrays. Throughout the simulations, there are $Q = 50$ pulses in a single CPI. We assume that there are $L = 3$ targets with $\{\theta_l\}_{l=1}^{L}$ in linear array case and $\{(\theta_l, \varphi_l)\}_{l=1}^{L}$ in planar array case. The normalized Doppler shifts are $f_1 = -0.1, f_2 = 0.2$ and $f_3 = 0.2$. The number of Monte Carlo trials is $P = 200$. The RCS of every target is drawn from a standard Gaussian distribution, and obeys the Swerling I model. Note that the last two targets share identical Doppler shifts, which causes the matrix $\mathbf{X}$ to drop rank. The noise signals are assumed to be Gaussian, zero-mean and white both temporally and spatially. The K orthogonal waveforms are $S_k(t) = \sqrt{\frac{1}{T}} e^{j2\pi\frac{k}{T}t}$, $k = 1, \ldots, K$. The tensor model in (22) is used and the TB matrix is pre-designed [6], [31].

For the case of linear array, we assume a transmit ULA with $S = 8$ subarrays. Each transmit subarray has $M_0 = 10$ elements spaced at half the wavelength. The placement of transmit subarrays can vary from totally overlapped case to non-overlapped case. The number of transmit elements is computed by $M = M_0 + \Delta_s(S-1)$. The receive array has $N = 12$ elements, which are randomly selected from the elements of the transmit array.

For the case of planar array, the reference transmit subarray is a 7×7 URA. The number of subarrays is $S = 6$, where $J = 2$ and $I = 3$. The distances between subarrays in both directions are fixed as the working wavelength, which means that $\Delta_x = 2$ and $\Delta_y = 2$. As for the planar array case, the receive array has $N = 12$ elements, which are randomly selected from the elements of the transmit array.

Signal covariance matrix-based DOA estimation methods as well as other signal tensor decomposition-based DOA estimation methods are introduced for comparison. The signal covariance matrix-based DOA estimation methods contain ESPRIT algorithm [8] and U-ESPRIT algorithm [10], while the signal tensor decomposition-based DOA estimation methods include CP-ESPRIT [11], [19] and HOSVD-ESPRIT [14], [16]. The Cramer-Rao bound (CRB) for MIMO radar is also provided.

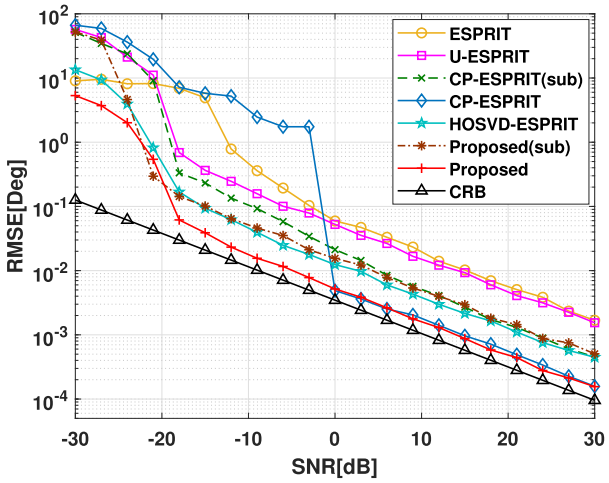

Fig. 2. RMSE versus SNR for 1-D TB MIMO radar.

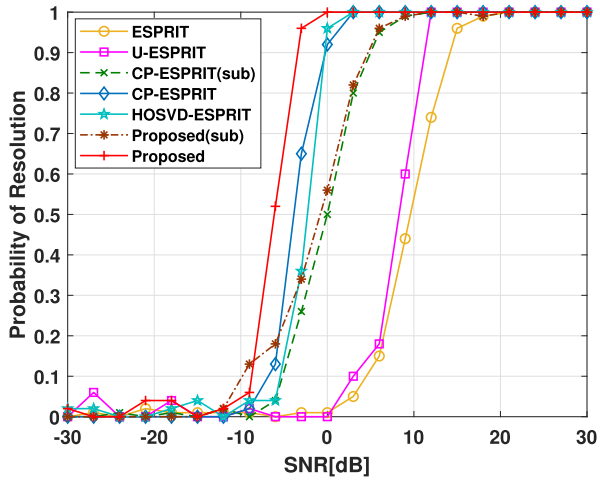

Fig. 3. Resolution versus SNR for 1-D TB MIMO radar.

Note that the HOSVD-ESPRIT method can only exploit the RIP among different transmit subarrays to conduct DOA estimation, while the CP-ESPRIT approach and our proposed algorithm can estimate targets DOA from both the first and second factor matrices. For targets DOA estimated by the second factor matrix $\mathbf{C}$, if applicable, we use a postfix to distinguish it, e.g., CP-ESPRIT(sub) refers to the estimation result computed by $\mathbf{C}$, while CP-ESPRIT denotes the estimation result originated from the first factor matrix after tensor decomposition.

A. Example 1: RMSE and Probability of Resolution for ULA With Partly Overlapped Subarrays ($\Delta_s = 6$)

Three targets are placed at $\theta_l \in \{-15^\circ, 5^\circ, 15^\circ\}$. Consider the matricized form of $\mathcal{Z}$ in (24). The goal is to estimate θ_l from $\mathbf{Z} = \mathbf{T} + \tau\mathbf{R}$. The SNR is measured as: $\mathrm{SNR[dB]} = 10\log(\|\mathbf{T}_{(3)}\|_F^2/\|\tau\mathbf{R}\|_F^2)$. The RMSE is computed by

$$RMSE = \sqrt{\frac{1}{2PL}\sum_{l=1}^{L}\sum_{p=1}^{P}\left(\hat{\theta}_l(p) - \theta_l(p)\right)^2}. \tag{49}$$

As shown in Fig. 2, the RMSEs decline gradually with the rise of SNR for all methods. The ESPRIT-based algorithm merely exploits the phase rotations between transmit subarrays and the performance is quite poor. U-ESPRIT algorithm performs better since the number of snapshots is doubled. The designed tensor model enables us to take advantage of the multi-dimensional structure of the received signal. The HOSVD-ESPRIT method, which utilizes the orthogonality between signal subspace and noise subspace in tensor form, improves the estimation accuracy. However, it suffers from the rank deficiency problem in $\mathbf{X}$ and requires extra preprocessing like spatial smoothing [41]. For the CP-ESPRIT approach and the proposed method, targets angular information can be obtained from both factor matrices $\mathbf{D}$ and $\mathbf{C}$, which are used to compare to each other in order to eliminate the potential grating lobes. The rank deficiency is also solved. The proposed method approaches the CRB with a lower threshold as compared to other tensor decomposition-based methods. It is because the Vandermonde structure of the factor matrix is exploited. Note that the computational complexity of our proposed method is reduced significantly. Indeed, it requires approximately the same number of flops as it is required in a single iteration of the CP-ESPRIT method. Also, the comparison of the estimation results between the first factor and second factor matrices shows a reasonable difference. This is mainly caused by the difference between the apertures of the transmit subarray and the whole transmit array.

For the probability of resolution, we assume only two closely spaced targets located at $\theta_l \in \{-5^\circ, -6^\circ\}$. These two targets are considered to be resolved when $\|\hat{\theta}_l - \theta_l\| \le \|\theta_1 - \theta_2\|/2,\ l = 1, 2$. The Doppler shifts are both $f = 0.2$ and the other parameters are the same as before.

In Fig. 3, the probability of resolution results for all methods tested are shown and they are consistent with those in Fig. 2. All methods achieve absolute resolution in high SNR region, and the resolution declines with the decrease of SNR. The ESPRIT method presents the worst performance while performance of the U-ESPRIT improves slightly. The results of the CP-ESPRIT(sub) method and the Proposed(sub) method are almost the same. The HOSVD-ESPRIT approach and the CP-ESPRIT method perform better, while the proposed method performs the best. Indeed, a gap of approximately 3 dB SNR can be observed between the proposed method and other tensor decomposition-based methods, which means that our proposed method enables the lowest SNR threshold. The performance of the proposed method in terms of both accuracy and resolution surpasses that of the other methods because the shift-invariances between and within different transmit subarrays are fully exploited.

B. Example 2: RMSE and Probability of Resolution for URA With Partly Overlapped Subarrays ($\Delta_x = \Delta_y = 2$)

In this example, three targets are placed at $(\theta_l, \varphi_l) \in \{(-40^\circ, 25^\circ), (-30^\circ, 35^\circ), (-20^\circ, 45^\circ)\}$. The signal model $\mathbf{Z} = \mathbf{T} + \tau\mathbf{R}$ is applied, where $\mathbf{T}$ is given by (28). The SNR is measured in the same way as that in the previous example for linear array. The RMSE for the case of planar array is computed

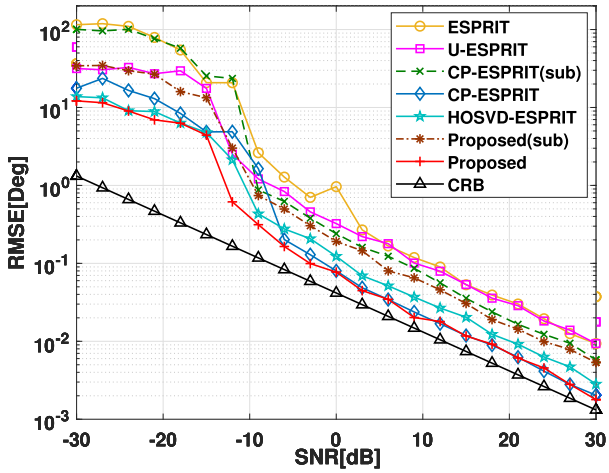

Fig. 4. RMSE versus SNR for two-dimensional TB MIMO radar.

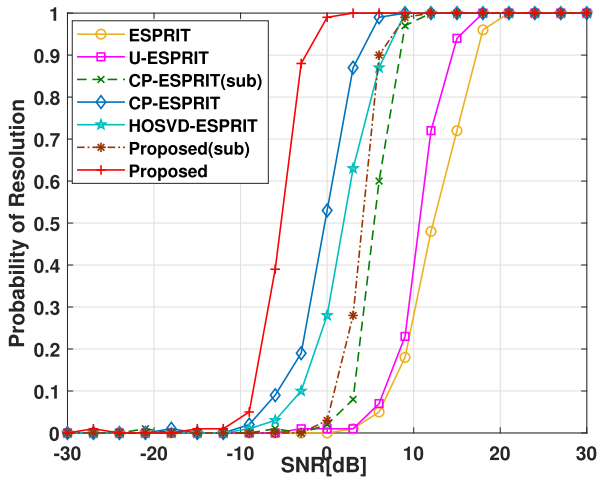

Fig. 5. Resolution versus SNR for two-dimensional TB MIMO radar.

as

$$RMSE = \sqrt{\frac{1}{2PL}\sum_{l=1}^{L}\sum_{p=1}^{P}\left[\left(\hat{\theta}_l(p)-\theta_l(p)\right)^2+\left(\hat{\varphi}_l(p)-\varphi_l(p)\right)^2\right]}. \tag{50}$$

In Fig. 4, the RMSEs of ESPRIT, U-ESPRIT, HOSVD-ESPRIT, CP-ESPRIT and the proposed method are given. The CRB is also provided. The ESPRIT and U-ESPRIT methods perform relatively poor. It is because the received signal shift-invariance within a single transmit subarray is ignored by these methods. Then we use the designed tensor model to conduct DOA estimation via tensor decomposition. The HOSVD-ESPRIT method exploits the RIP among different transmit subarrays via HOSVD and achieves a better DOA estimation accuracy as compared to the two aforementioned signal covariance matrix-based methods. It can be observed that the Proposed(sub) and CP-ESPRIT(sub) successfully estimate the targets DOA via $\mathbf{C}$ in the case of planar array, which proves the validity of (37). The results can be used to mitigate the spatial ambiguity in the following estimations. Like their counterparts in linear array case, the RMSEs of the proposed method and the CP-ESPRIT method are almost the same for above 0 dB SNR and they surpass that of the HOSVD-ESPRIT method. The performance of the HOSVD-ESPRIT is degraded slightly due to the spatial smoothing introduced for solving rank deficiency problem in $\mathbf{X}$. The CP-ESPRIT method ignores the Vandermonde structure of factor matrix during tensor decomposition, while the proposed approach fully exploits the Vandermonde factor matrix to improve the DOA estimation performance.

To evaluate the resolution performance, only two targets are reserved and the spatial directions are $(\theta_l, \varphi_l) \in \{(-10^\circ, 15^\circ), (-11^\circ, 16^\circ)\}$. The resolution is considered successful if $\|\hat{\theta}_l - \theta_l\| \leq \|\theta_1 - \theta_2\|/2$, $\|\hat{\varphi}_l - \varphi_l\| \leq \|\varphi_1 - \varphi_2\|/2$, $l = 1, 2$. The target Doppler shifts are the same, given as $f = 0.2$. The other parameters are unchanged.

Fig. 5 shows the results for all methods tested with respect to the probability of resolution. The proposed method achieves the lowest SNR threshold. This is the result of exploiting fully the shift-invariances between and within different transmit subarrays and the Vandermonde structure during tensor decomposition. Since the two targets have identical Doppler shifts, the HOSVD-ESPRIT requires extra preprocessing and leads to performance loss. The convergence of the CP-ESPRIT method is unstable and can be affected by the tensor size. It can be observed that the resolution performance of the CP-ESPRIT method is deteriorated as compared to its counterpart in Fig. 3. This implies that the robustness of our proposed method is better for 2-D DOA estimation because no iterations are required.

C. Example 3: RMSE Performance for ULA With Different Δ_s

In this example, we are concerned with the RMSE performance when Δ_s changes from one to at most M_0 for TB MIMO radar with ULA transmit subarrays. The aperture is increased gradually. The SNR is assumed to be 10 dB. All other parameters are the same as those in Example 1. Given the number of subarrays and the structure of a single subarray, the aperture of the overall transmit ULA rises with the increase of Δ_s while the number of elements shared by two adjacent subarrays declines. When $\Delta_s = 0$, this model is identical to that for the conventional ESPRIT method [6], [31], and there is no transmit subarray. When Δ_s rises, the distance between phase centers for two adjacent subarrays becomes larger than half the working wavelength and grating lobes are generated. These grating lobes can be eliminated. Meanwhile, the transmit array aperture is increased and the DOA estimation performance should be improved. To evaluate the performance, the RMSEs of DOA estimations obtained by different methods tested are computed versus Δ_s.

It can be seen in Fig. 6 that the RMSEs for all methods tested decrease steadily with the increase of Δ_s. The ESPRIT and U-ESPRIT methods suffer from grating lobes and the received signal within a single subarray is not fully exploited, hence, they perform poorly. The HOSVD-ESPRIT method improves the performance significantly, since tensor model is utilized. Meanwhile, the estimation performance of the HOSVD-ESPRIT

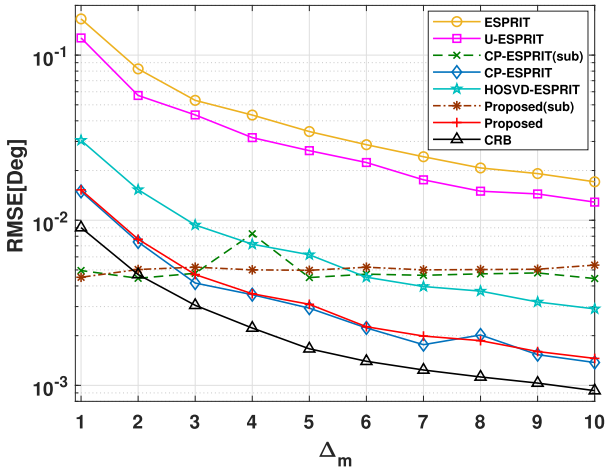

Fig. 6. RMSE versus Δ_s for 1-D TB MIMO radar.

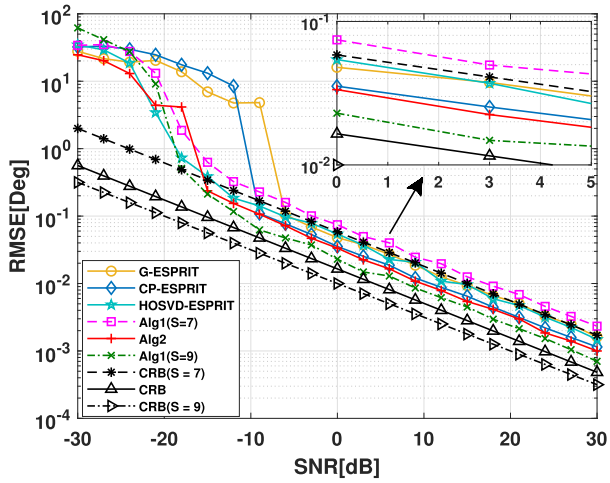

Fig. 7. RMSE versus SNR for 1-D TB MIMO radar with non-uniformly spaced transmit subarrays.

method is worse than that of the CP-ESPRIT approach and the proposed method. The spatial smoothing is used to tackle the rank deficiency problem in signal subspace. The RMSEs of the Proposed(sub) and the CP-ESPRIT(sub) are almost unchanged as the estimation is only based on a single transmit subarray, which is fixed during the simulation. It can be noted in Fig. 2 that the CRB is nearly achieved by the CP-ESPRIT method and our proposed method. Consequently, the RMSEs of the proposed method and the CP-ESPRIT method are nearly Coincide.

To evaluate the RMSE performance versus Δ_x or Δ_y for TB MIMO radar with URA transmit subarrays, it is necessary to separately add a new subarray in one direction while keeping the array structure in the other direction unchanged. This can be fulfilled by constructing an L-shaped transmit array, where each element is replaced by a URA subarray. However, this analysis would be beyond the scope of this paper. In general, it can be concluded that the proposed method can estimate the targets DOA via the phase rotations between transmit subarrays. If the placement of two adjacent transmit subarrays satisfies some conditions, e.g., $\Delta_s > 3$ for the linear array case, the RMSE performance is better than that computed by a single transmit subarray.

D. Example 4: RMSE Performance for Non-Uniformly Spaced Transmit Subarrays With $m_s \in \{1, 2, 3, 5, 7, 9\}$

In this example, we evaluate the RMSE performance of the proposed DOA estimation method for TB MIMO radar with non-uniformly spaced transmit subarrays. Consider a TB MIMO radar with linear array. The transmit linear array has $S = 7$ subarrays with $m_s \in \{1, 2, 3, 5, 6, 7, 9\}$. Each subarray contains $M_0 = 10$ elements. The receive array is formed by randomly selecting $N = 12$ elements from the transmit array. Three targets are placed at $\theta_1 = -5°, \theta_2 = 10°$ and $\theta_3 = 18°$ with normalized Doppler shifts $f_1 = 0.3$, $f_2 = -0.15$ and $f_3 = -0.15$. To simplify the signal model, we assume that each subarray is a ULA, which is not used during the DOA estimation in this example. Then Algorithm 2 can be applied, since the subarray structure stays identical. Two different transmit arrays are introduced for comparison to illustrate the improved performance provided by constructing $\mathbf{D}^{(\mathrm{sub})}$. Both of them can be regarded as a linear array with uniformly spaced transmit subarrays ($\Delta_s = 1$). The first one has $S = 7$ subarrays, while the second one has $S = 9$ subarrays to achieve the same aperture. The DOA estimation for these two transmit arrays can be conducted via Algorithm 1. The generalized-ESPRIT (G-ESPRIT) method of [44] and the HOSVD-ESPRIT approach that uses the same tensor model (43) as the proposed method are used for comparison. The CRBs for models corresponding to three different transmit arrays are also shown.

From Fig 7, it can be observed that by constructing $\mathbf{D}^{(\mathrm{sub})}$ we are able to exploit the multiple scales of shift-invariances in the generalized Vandermonde factor matrix. By solving (48), the grating lobes are eliminated efficiently. Hence, the structure of transmit subarrays can be arbitrary but identical, which provides more flexibility for array design. The RMSE of the proposed approach surpasses those of the G-ESPRIT, HOSVD-ESPRIT and CP-ESPRIT methods. Also, the performance of the non-uniformly spaced transmit subarrays is better than that of the uniformly spaced transmit subarrays (S = 7). This is expected since the aperture is increased due to sparsity. Compared to the fully spaced transmit subarrays case (S = 9), the performance of the proposed method is deteriorated slightly. However, the fully spaced array can be extremely high-cost if the array aperture is further increased. By using the generalized Vandermonde matrix, the proposed method enables the sparsity in the transmit array, and it helps to achieve higher resolution with less elements.

E. Example 5: RMSE Performance for Arbitrary but Identical Transmit Subarrays

In this example, we illustrate the performance of the proposed DOA estimation method for TB MIMO radar with arbitrary but identical subarrays. Specifically, a planar array with $S = 4 \times 4$ subarrays is considered, whose phase centers form a uniform rectangular grid with a distance of half the working wavelength. For each subarray, $M_0 = 4$ elements are randomly placed in a circle centered on the phase center with a radius of a quarter of wavelength. All subarrays have identical structure,

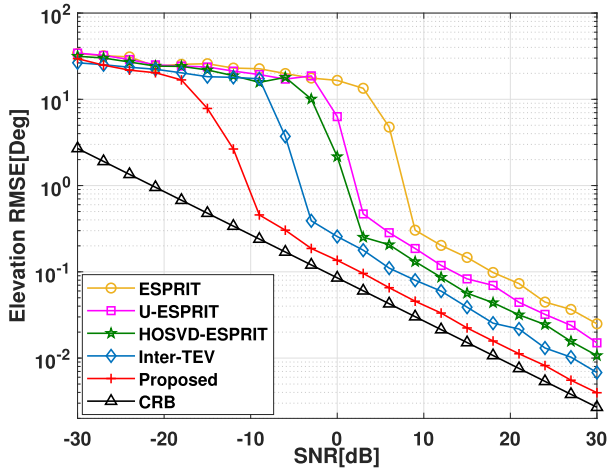

(a) Elevation RMSE versus SNR

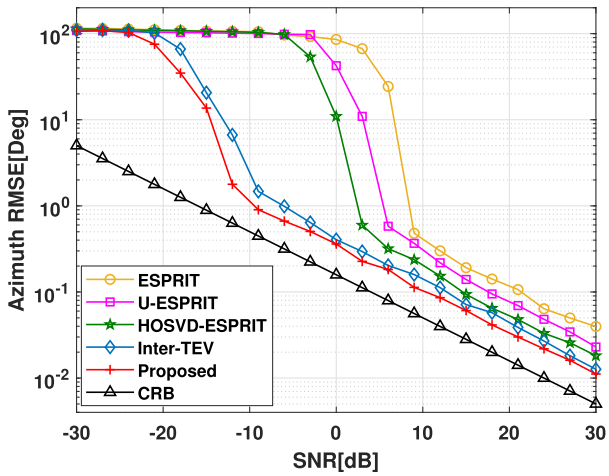

(b) Azimuth RMSE versus SNR

Fig. 8. RMSE versus SNR for 2-D TB MIMO radar with arbitrary but identical transmit subarrays.

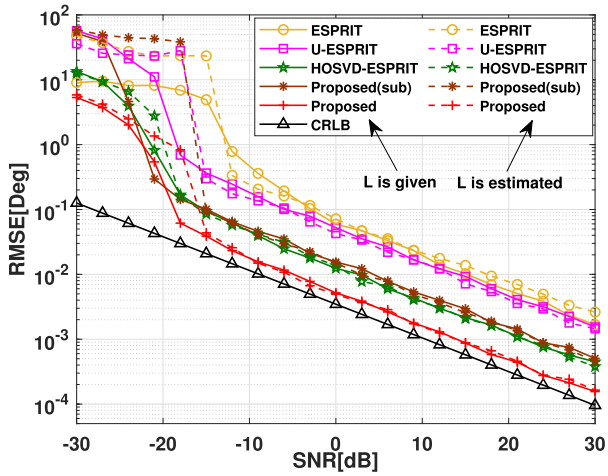

(a) 1-D case; the number of targets is estimated

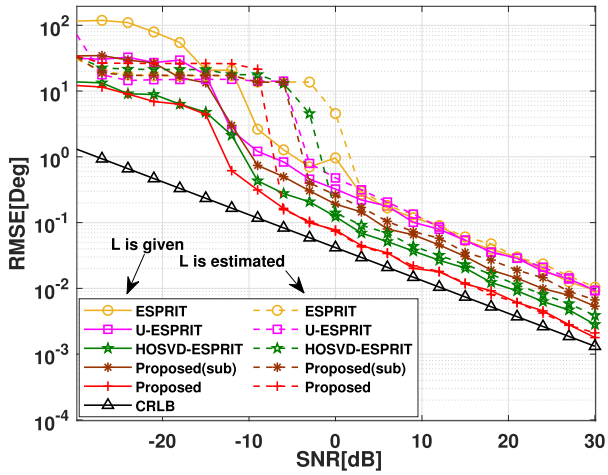

(b) 2-D case; the number of targets is estimated

Fig. 9. RMSE versus SNR; the transmit subarrays are uniformly spaced.

hence, the targets DOA can be estimated using Algorithm 2. The receive array is formed by randomly selecting $N = 12$ elements from the transmit array. Three targets are placed at $(\theta_l, \varphi_l) \in \{(-26°, 11°), (-19°, 21°), (-12°, 31°)\}$. The other parameters are the same as those in Example 2.

Note that the subarray is arbitrary, and the DOA parameters can only be estimated by the phase rotations between the transmit subarrays. The ESPRIT and U-ESPRIT methods are used as representatives of the signal covariance matrix-based methods while the HOSVD-ESPRIT is utilized as a representative of the signal tensor decomposition-based methods. As another existing alternative approach, the transmit array interpolation technique of [14] has been introduced to map the original transmit array into a URA (in our example here, 4×4 URA) to enable the Tensor-ESPRIT-based DOA estimation. We refer to this method as Inter-TEV method in Fig. 8. It can be observed from the figures that by carefully designing the mapping matrix, the RMSEs of the Inter-TEV method are better than those of the ESPRIT, U-ESPRIT and HOSVD-ESPRIT methods for both elevation and azimuth angles estimation. The proposed method surpasses the other methods, including the Inter-TEV method, and shows the lowest RMSE. This is because of the full usage of the shift-invariance between and within different transmit subarrays.

F. Example 6: RMSE Performance With Estimated Number of Targets for 1-D and 2-D Cases

In the final example, we evaluate the RMSE performance of the estimated number of targets described in Section III-D. The RMSEs of the aforementioned DOA estimation methods, if applicable, are also shown for comparison. Note that only the CP-ESPRIT method is not compared because it requires the targets number as an input to initialize the ALS algorithm. The signal models in Example 1 for 1-D case and Example 2 for 2-D case are utilized, respectively. The results are given in Fig. 9. The dotted lines are used for the case of estimated number of targets, while the solid lines correspond to the case when L is precisely known. It can be seen that an inaccurate estimation of L leads to increasing the RMSEs for all methods, and it happens only in low SNR region. If SNR is large enough (e.g., larger than -15 dB for the 1-D case and -9 dB for the 2-D case), the number of targets is estimated correctly. Then, the RMSE performance

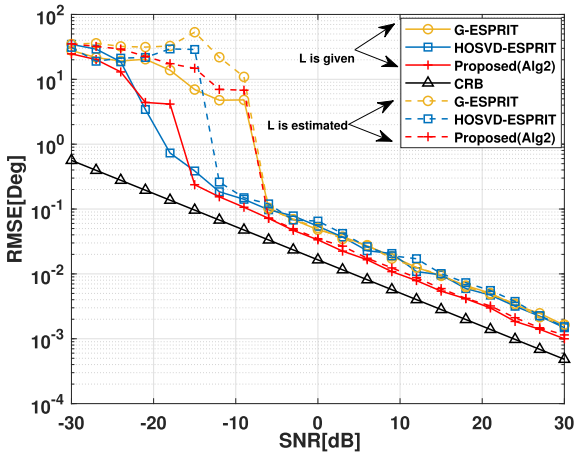

Fig. 10. RMSE versus SNR for 1-D TB MIMO radar; non-uniformly spaced transmit subarrays, the number of targets is estimated.

with estimated L is nearly the same as that with the precise L. It is worth stressing that the proposed approach achieves the lowest RMSE in both scenarios.

The non-uniform case is also considered in Fig. 10 as an extension to Example 4 (here the G-ESPRIT and HOSVD-ESPRIT methods are used for comparison). A similar conclusion as for the uniform case can be made. The influence of inaccurate estimation of L on DOA estimation performance is secondary as compared to the influence of low SNR itself, since the DOA estimation accuracy is limited in low SNR region even when the correct number of targets is known.

VI. Conclusion

The problem of tensor decomposition with Vandermonde factor matrix in application to DOA estimation for TB MIMO radar with transmit subarrays has been considered. A general higher-order tensor that can be used to express the TB MIMO radar received signal in a variety of scenarios, e.g., linear and planar arrays, uniformly and non-uniformly spaced subarrays, regular and irregular subarrays, has been designed. The shift-invariance of the received signal between and within different transmit subarrays have been used to conduct DOA estimation. Specifically, a computationally efficient tensor decomposition method has been proposed to estimate the generators of the Vandermonde factor matrices, which can be used in the form of a look-up table for finding targets DOA. The proposed method fully exploits the shift-invariance of the received signal between and within different transmit subarrays, and it can be regarded as a generalized tensor decomposition-based ESPRIT method. Comparing with conventional signal tensor decomposition-based techniques like CP-ESPRIT and HOSVD-ESPRIT methods, our proposed method takes advantage of the Vandermonde structure of factor matrices, and it requires no iterations. The parameter identifiability of our tensor model has also been studied via the discussion of the uniqueness condition for the signal tensor decomposition. Simulation results have verified that the proposed DOA estimation method has better accuracy and higher resolution as compared to existing techniques for TB MIMO radar DOA estimation.

Appendix A
Proof of Lemma 1

First, note that $r(\mathbf{A}^{(3)}) = L$ since $\mathbf{A}^{(3)}$ is a tall matrix with column full rank. Then note that $\mathbf{A}^{(1)} \odot \mathbf{A}^{(2)} = \mathbf{B} \odot \mathbf{C} \odot \mathbf{A}^{(2)} = \mathbf{\Pi}(\mathbf{B} \odot \mathbf{A}^{(2)} \odot \mathbf{C})$ where $\mathbf{\Pi}$ is an exchange matrix. Here the KR product $\mathbf{B} \odot \mathbf{A}^{(2)}$ of a Vandermonde matrix and an arbitrary matrix has the rank $\min\{pI_2, L\}$ (see [20], [21]), and $r(\mathbf{B} \odot \mathbf{A}^{(2)} \odot \mathbf{C}) = \min\{I_1 I_2, L\}$. Since $\mathbf{\Pi}$ is nonsingular, $r(\mathbf{B} \odot \mathbf{C} \odot \mathbf{A}^{(2)}) = r(\mathbf{B} \odot \mathbf{A}^{(2)} \odot \mathbf{C}) = \min\{I_1 I_2, L\}$. Using this property, we have $r(\overline{\mathbf{B}} \odot \mathbf{C} \odot \mathbf{A}^{(2)}) = r(\underline{\mathbf{B}} \odot \mathbf{C} \odot \mathbf{A}^{(2)}) = r(\underline{\mathbf{B}} \odot \mathbf{A}^{(2)} \odot \mathbf{C}) = \min\{(p-1)qI_2, L\} = L$ and $r(\mathbf{B} \odot \overline{\mathbf{C}} \odot \mathbf{A}^{(2)}) = r(\mathbf{B} \odot \underline{\mathbf{C}} \odot \mathbf{A}^{(2)}) = \min\{(q-1)pI_2, L\} = L$.

Next, consider the 3-th multi-mode unfolding of $\mathcal{Y}$, which is given by $\mathbf{Y}_{(3)} = (\mathbf{A}^{(1)} \odot \mathbf{A}^{(2)})(\mathbf{A}^{(3)})^T$. The SVD of this matrix is $\mathbf{Y}_{(3)} = \mathbf{U}\mathbf{\Lambda}\mathbf{V}^H$, where $\mathbf{U} \in \mathbb{C}^{I_1 I_2 \times L}$, $\mathbf{\Lambda} \in \mathbb{C}^{L \times L}$, and $\mathbf{V} \in \mathbb{C}^{I_3 \times L}$. Since $r(\mathbf{A}^{(3)}) = L$, it can be derived that a nonsingular matrix $\mathbf{E} \in \mathbb{C}^{L \times L}$ satisfies $\mathbf{U}\mathbf{E} = \mathbf{B} \odot \mathbf{C} \odot \mathbf{A}^{(2)}$, i.e.,

$$\begin{aligned} &\mathbf{U}_2\mathbf{E} = \underline{\mathbf{B}} \odot \mathbf{C} \odot \mathbf{A}^{(2)}, \quad \mathbf{U}_1\mathbf{E} = \overline{\mathbf{B}} \odot \mathbf{C} \odot \mathbf{A}^{(2)} \\ &\mathbf{U}_4\mathbf{E} = \mathbf{B} \odot \underline{\mathbf{C}} \odot \mathbf{A}^{(2)}, \quad \mathbf{U}_3\mathbf{E} = \mathbf{B} \odot \overline{\mathbf{C}} \odot \mathbf{A}^{(2)}, \end{aligned} \tag{51}$$

where the submatrices $\mathbf{U}_1$, $\mathbf{U}_2$, $\mathbf{U}_3$ and $\mathbf{U}_4$ are truncated from rows of $\mathbf{U}$ according to the operator of the KR product, i.e.,

$$\begin{aligned} \mathbf{U}_1 &= \left[\mathbf{I}_{qI_2(p-1)}, \mathbf{0}_{qI_2(p-1)\times qI_2}\right] \mathbf{U} \\ \mathbf{U}_2 &= \left[\mathbf{0}_{qI_2(p-1)\times qI_2}, \mathbf{I}_{qI_2(p-1)}\right] \mathbf{U} \\ \mathbf{U}_3 &= \left(\mathbf{I}_p \otimes \left[\mathbf{I}_{I_2(q-1)}, \mathbf{0}_{I_2(q-1)\times I_2}\right]\right) \mathbf{U} \\ \mathbf{U}_4 &= \left(\mathbf{I}_p \otimes \left[\mathbf{0}_{I_2(q-1)\times I_2}, \mathbf{I}_{I_2(q-1)}\right]\right) \mathbf{U}. \end{aligned} \tag{52}$$

By exploiting the Vandermonde structure of $\mathbf{B}$ and $\mathbf{C}$, we have $\mathbf{U}_2\mathbf{E} = \mathbf{U}_1\mathbf{E}\mathbf{\Omega}_b$ and $\mathbf{U}_4\mathbf{E} = \mathbf{U}_3\mathbf{E}\mathbf{\Omega}_c$, where $\mathbf{\Omega}_b = diag(\boldsymbol{\omega}_b)$, $\mathbf{\Omega}_c = diag(\boldsymbol{\omega}_c)$ with $\boldsymbol{\omega}_b$ and $\boldsymbol{\omega}_c$ denoting the vectors of generators of $\mathbf{B}$ and $\mathbf{C}$, respectively. Note that $\mathbf{E}$, $\mathbf{\Omega}_b$ and $\mathbf{\Omega}_c$ are full rank. We have $\mathbf{U}_1^{\dagger}\mathbf{U}_2 = \mathbf{E}\mathbf{\Omega}_b\mathbf{E}^{-1}$ and $\mathbf{U}_3^{\dagger}\mathbf{U}_4 = \mathbf{E}\mathbf{\Omega}_c\mathbf{E}^{-1}$. Hence, the vectors $\boldsymbol{\omega}_b$ and $\boldsymbol{\omega}_c$ can be computed as the collections of eigenvalues of $\mathbf{U}_1^{\dagger}\mathbf{U}_2$ and $\mathbf{U}_3^{\dagger}\mathbf{U}_4$, respectively, while $\mathbf{E}$ is the collection in the matrix form of the corresponding eigenvectors. From the generators of $\mathbf{B}$ and $\mathbf{C}$, the first factor matrix $\mathbf{A}^{(1)}$ can be reconstructed column by column, i.e., $\mathbf{a}_l^{(1)} = \mathbf{b}_l \odot \mathbf{c}_l$, where $\mathbf{a}_l^{(1)}$, $\mathbf{b}_l$ and $\mathbf{c}_l$ are the l-th column of $\mathbf{A}^{(1)}$, $\mathbf{B}$ and $\mathbf{C}$, respectively.

Using the fifth relationship in (1), we have

$$\mathbf{a}_l^{(2)} = \left(\frac{\left(\mathbf{a}_l^{(1)}\right)^H}{\left(\mathbf{a}_l^{(1)}\right)^H \mathbf{a}_l^{(1)}} \otimes \mathbf{I}_{I_2}\right)\left(\mathbf{a}_l^{(1)} \otimes \mathbf{a}_l^{(2)}\right), \tag{53}$$

where $\mathbf{a}_l^{(2)}$ is the l-th column of $\mathbf{A}^{(2)}$. It can also be observed that $\mathbf{a}_l^{(1)} \otimes \mathbf{a}_l^{(2)} = \mathbf{b}_l \odot \mathbf{c}_l \odot \mathbf{a}_l^{(2)}$, which is the l-th column of the matrix $\mathbf{A}^{(1)} \odot \mathbf{A}^{(2)}$. From (51), we have $\mathbf{a}_l^{(1)} \otimes \mathbf{a}_l^{(2)} = \mathbf{U}\mathbf{e}_l$,

where $\mathbf{e}_l$ is the l-th column of the nonsingular matrix $\mathbf{E}$. Substituting it into (53) and assuming that the column vectors of $\mathbf{A}^{(1)}$ have unit norm, $\mathbf{a}_l^{(2)}$ can be computed by

$$\mathbf{a}_l^{(2)} = \left(\left(\mathbf{a}_l^{(1)}\right)^H \otimes \mathbf{I}_{I_2}\right)\mathbf{U}\mathbf{e}_l, \quad l = 1, 2, \ldots, L. \tag{54}$$

Using $\mathbf{A}^{(1)}$ and $\mathbf{A}^{(2)}$, the third factor matrix is given as

$$\left(\boldsymbol{A}^{(3)}\right)^T = \left(\left(\left(\boldsymbol{A}^{(1)}\right)^H \mathbf{A}^{(1)}\right) * \left(\left(\boldsymbol{A}^{(2)}\right)^H \mathbf{A}^{(2)}\right)\right)^{-1} \times \left(\mathbf{A}^{(1)} \odot \mathbf{A}^{(2)}\right)^H \mathbf{Y}_{(3)}. \tag{55}$$

Therefore, the tensor decomposition of $\mathcal{Y}$ is generally unique. This completes the proof.

In the particular case of $\mathbf{A}^{(1)} \in \mathbb{C}^{I_1 \times L}$ being reduced to a Vandermonde matrix with distinct generators, the decomposition of $\mathcal{Y}$ is unique if $(I_1 - 1)I_2 \geq L$. This can be also verified by Proposition III.2 in [20] or Theorem 1.13 in [35].

REFERENCES

[1] A. M. Haimovich, R. S. Blum, and L. J. Cimini, "MIMO radar with widely separated antennas," *IEEE Signal Process. Mag.*, vol. 25, no. 1, pp. 116–129, Jan. 2008.

[2] J. Li and P. Stoica, "MIMO radar with colocated antennas," *IEEE Signal Process. Mag.*, vol. 24, no. 5, pp. 106–114, Sep. 2007.

[3] A. Hassanien and S. A. Vorobyov, "Transmit energy focusing for DOA estimation in MIMO radar with colocated antennas," *IEEE Trans. Signal Process.*, vol. 59, no. 6, pp. 2669–2682, Jun. 2011.

[4] A. Hassanien and S. A. Vorobyov, "Phased-MIMO radar: A tradeoff between phased-array and MIMO radars," *IEEE Trans. Signal Process.*, vol. 58, no. 6, pp. 3137–3151, Jun. 2010.

[5] D. R. Fuhrmann, J. P. Browning, and M. Rangaswamy, "Signaling strategies for the hybrid MIMO phased-array radar," *IEEE J. Sel. Topics Signal Process.*, vol. 4, no. 1, pp. 66–78, Feb. 2010.

[6] A. Khabbazibasmenj, A. Hassanien, S. A. Vorobyov, and M. W. Morency, "Efficient transmit beamspace design for search-free based DOA estimation in MIMO radar," *IEEE Trans. Signal Process.*, vol. 62, no. 6, pp. 1490–1500, Mar. 2014.

[7] Z. Guo, X. Wang, and W. Heng, "Millimeter-wave channel estimation based on 2-D beamspace MUSIC method," *IEEE Trans. Wireless Commun.*, vol. 16, no. 8, pp. 5384–5394, Aug. 2017.

[8] A. Hu, T. Lv, H. Gao, Z. Zhang, and S. Yang, "An ESPRIT-based approach for 2-D localization of incoherently distributed sources in massive MIMO systems," *IEEE J. Sel. Topics Signal Process.*, vol. 8, no. 5, pp. 996–1011, Oct. 2014.

[9] N. Tayem and H. M. Kwon, "L-shape 2-dimensional arrival angle estimation with propagator method," *IEEE Trans. Antennas Propag.*, vol. 53, no. 5, pp. 1622–1630, May 2005.

[10] M. D. Zoltowski, M. Haardt, and C. P. Mathews, "Closed-form 2-D angle estimation with rectangular arrays in element space or beamspace via unitary ESPRIT," *IEEE Trans. Signal Process.*, vol. 44, no. 2, pp. 316–328, Feb. 1996.

[11] D. Nion and N. D. Sidiropoulos, "Tensor algebra and multidimensional harmonic retrieval in signal processing for MIMO radar," *IEEE Trans. Signal Process.*, vol. 58, no. 11, pp. 5693–5705, Nov. 2010.

[12] B. Xu, Y. Zhao, Z. Cheng, and H. Li, "A novel unitary PARAFAC method for DOD and DOA estimation in bistatic MIMO radar," *Signal Process.*, vol. 138, pp. 273–279, Sep. 2017.

[13] N. Sidiropoulos, R. Bro, and G. Giannakis, "Parallel factor analysis in sensor array processing," *IEEE Trans. Signal Process.*, vol. 48, no. 8, pp. 2377–2388, Aug. 2000.

[14] M. Cao, S. A. Vorobyov, and A. Hassanien, "Transmit array interpolation for DOA estimation via tensor decomposition in 2-D MIMO radar," *IEEE Trans. Signal Process.*, vol. 65, no. 19, pp. 5225–5239, Oct. 2017.

[15] L. De Lathauwer, B. De Moor, and J. Vandewalle, "A multilinear singular value decomposition," *SIAM J. Matrix Anal. Appl.*, vol. 21, no. 4, pp. 1253–1278, 2000.

[16] M. Haardt, F. Roemer, and G. D. Galdo, "Higher-order SVD-based subspace estimation to improve the parameter estimation accuracy in multidimensional harmonic retrieval problems," *IEEE Trans. Signal Process.*, vol. 56, no. 7, pp. 3198–3213, Jul. 2008.

[17] S. D. Blunt and E. L. Mokole, "Overview of radar waveform diversity," *IEEE Trans. Aerosp. Electron. Syst.*, vol. 31, no. 11, pp. 2–42, Nov. 2016.

[18] A. Hassanien, M. W. Morency, A. Khabbazibasmenj, S. A. Vorobyov, J. Park, and S. Kim, "Two-dimensional transmit beamforming for MIMO radar with sparse symmetric arrays," in *Proc. IEEE Radar Conf.*, Ottawa, ON, Canada, 2013, pp. 1–6.

[19] N. D. Sidiropoulos *et al.*, "Tensor decomposition for signal processing and machine learning," *IEEE Trans. Signal Process.*, vol. 65, no. 13, pp. 3551–3582, Jul. 2017.

[20] M. Sørensen and L. D. Lathauwer, "Blind signal separation via tensor decomposition with vandermonde factor: Canonical polyadic decomposition," *IEEE Trans. Signal Process.*, vol. 61, no. 22, pp. 5507–5519, Nov. 2013.

[21] T. Jiang, N. D. Sidiropoulos, and J. M. F. ten Berge, "Almost-sure identifiability of multidimensional harmonic retrieval," *IEEE Trans. Signal Process.*, vol. 49, no. 9, pp. 1849–1859, Sep. 2001.

[22] F. Xu, S. A. Vorobyov, and X. Yang, "Joint DOD and DOA estimation in slow-time MIMO radar via PARAFAC decomposition," *IEEE Signal Process. Lett.*, vol. 27, pp. 1495–1499, Aug. 2020.

[23] A. Cichocki *et al.*, "Tensor decompositions for signal processing applications: From two-way to multiway component analysis," *IEEE Signal Process. Mag.*, vol. 32, no. 2, pp. 145–163, Mar. 2015.

[24] F. Xu, X. Yang, and T. Lan, "Search-free direction-of-arrival estimation for transmit beamspace multiple-input multiple-output radar via tensor modelling and polynomial rooting," *IET Radar, Sonar Navigation*, vol. 15, no. 6, pp. 574–580, Apr. 2021.

[25] J. H. M. de Goulart, M. Boizard, R. Boyer, G. Favier, and P. Comon, "Tensor CP decomposition with structured factor matrices: Algorithms and performance," *IEEE J. Sel. Topics Signal Process.*, vol. 10, no. 4, pp. 757–769, Jun. 2016.

[26] W. Wang, H. C. So, and A. Farina, "An overview on time/frequency modulated array processing," *IEEE J. Sel. Topics Signal Process.*, vol. 11, no. 2, pp. 228–246, Mar. 2017.

[27] L. Lu, G. Y. Li, A. L. Swindlehurst, A. Ashikhmin, and R. Zhang, "An overview of massive MIMO: Benefits and challenges," *IEEE J. Sel. Topics Signal Process.*, vol. 8, no. 5, pp. 742–758, Oct. 2014.

[28] F. Xu and S. A. Vorobyov, "Constrained tensor decomposition for 2D DOA estimation in transmit beamspace MIMO radar with subarrays," in *Proc. 46th Int. Conf. Acoust., Speech, Signal Process.*, Toronto, Canada, 2021, pp. 4380–4384.

[29] A. L. F. de Almeida, G. Favier, and J. C. M. Mota, "Constrained tensor modeling approach to blind multiple-antenna CDMA schemes," *IEEE Trans. Signal Process.*, vol. 56, no. 6, pp. 2417–2428, Jun. 2008.

[30] H. Lin, C. Yuan, J. Du, and Z. Hu, "Estimation of DOA for noncircular signals via vandermonde constrained parallel factor analysis," *Int. J. Antennas Propag.*, vol. 2018, pp. 1–10, Jan. 2018.

[31] M. W. Morency and S. A. Vorobyov, "Partially adaptive transmit beamforming for search free 2D DOA estimation in MIMO radar," in *Proc. 23rd Eur. Signal Process. Conf.*, Nice, France, 2015, pp. 2631–2635.

[32] T. G. Kolda and B. W. Bader, "Tensor decompositions and applications," *SIAM Rev.*, vol. 51, no. 3, pp. 455–500, 2009.

[33] N. D. Sidiropoulos and R. Bro, "On the uniqueness of multilinear decomposition of N-way arrays," *J. Chemometrics*, vol. 14, no. 3, pp. 229–239, 2000.

[34] I. Domanov and L. D. Lathauwer, "On the uniqueness of the canonical polyadic decomposition of third-order tensors–Part II: Uniqueness of the overall decomposition," *SIAM J. Matrix Anal. Appl.*, vol. 34, no. 3, pp. 876–903, 2013.

[35] I. Domanov and L. De Lathauwer, "On the uniqueness of the canonical polyadic decomposition of third-order tensors–Part I: Basic results and uniqueness of one factor matrix," *SIAM J. Matrix Anal. Appl.*, vol. 34, no. 3, pp. 855–875, 2013.

[36] N. Sidiropoulos and X. Liu, "Identifiability results for blind beamforming in incoherent multipath with small delay spread," *IEEE Trans. Signal Process.*, vol. 49, no. 1, pp. 228–236, Jan. 2001.

[37] Z. Yang, P. Stoica, and J. Tang, "Source resolvability of spatial-smoothing-based subspace methods: A hadamard product perspective," *IEEE Trans. Signal Process.*, vol. 67, no. 10, pp. 2543–2553, May 2019.
[38] X. Guo, S. Miron, D. Brie, S. Zhu, and X. Liao, "A CANDECOMP/PARAFAC perspective on uniqueness of DOA estimation using a vector sensor array," *IEEE Trans. Signal Process.*, vol. 59, no. 7, pp. 3475–3481, Jul. 2011.
[39] X. Guo, S. Miron, D. Brie, and A. Stegeman, "Uni-mode and partial uniqueness conditions for CANDECOMP/PARAFAC of three-way arrays with linearly dependent loadings," *SIAM J. Matrix Anal. Appl.*, vol. 33, no. 1, pp. 111–129, 2012.
[40] Q.-T. Zhang, K. Wong, P. Yip, and J. Reilly, "Statistical analysis of the performance of information theoretic criteria in the detection of the number of signals in array processing," *IEEE Trans. Acoust., Speech, Signal Process.*, vol. 37, no. 10, pp. 1557–1567, Oct. 1989.
[41] M. Sørensen and L. De Lathauwer, "Multiple invariance ESPRIT for nonuniform linear arrays: A coupled canonical polyadic decomposition approach," *IEEE Trans. Signal Process.*, vol. 64, no. 14, pp. 3693–3704, Jul. 2016.
[42] A. L. Swindlehurst, B. Ottersten, R. Roy, and T. Kailath, "Multiple invariance esprit," *IEEE Trans. Signal Process.*, vol. 40, no. 4, pp. 867–881, Apr. 1992.
[43] K. V. Mishra, M. R. Bhavani Shankar, V. Koivunen, B. Ottersten, and S. A. Vorobyov, "Toward millimeter-wave joint radar communications: A signal processing perspective," *IEEE Signal Process. Mag.*, vol. 36, no. 5, pp. 100–114, Sep. 2019.
[44] B. Liao and S. Chan, "Direction-of-arrival estimation in subarrays-based linear sparse arrays with gain/phase uncertainties," *IEEE Trans. Aerosp. Electron. Syst.*, vol. 49, no. 4, pp. 2268–2280, Oct. 2013.

Feng Xu (Member, IEEE) received the Ph.D. degree in information and communication engineering from the School of Information and Electronics, Beijing Institute of Technology, Beijing, China, in 2021. From 2019 to 2021, he was a Visiting Doctoral Candidate with the Department of Signal Processing and Acoustics, Aalto University, Espoo, Finland, where he is currently a Research Assistant. His research interests include array signal processing, radar, and tensor decomposition.

Matthew W. Morency (Member, IEEE) received the B.Sc. degree in electrical engineering from the University of Alberta, Edmonton, AB, Canada, and the M.Sc. degree (with distinction) in electrical engineering from Aalto University, Espoo, Finland. From 2016 to 2020, he conducted Ph.D. studies with TU Delft. In late 2020, he began his career as an Engineer with Nokia Networks, Espoo, Finland. His research interests include signal processing, with specific focus on array processing, graph signal processing, and sparse sensing. He was the recipient of the 2015 IEEE CAMSAP Best Student Paper Award, and the NSERC Postgraduate Scholarship.

Sergiy A. Vorobyov (Fellow, IEEE) received the M.Sc. and Ph.D. degrees in systems and control from the Kharkiv National University of Radio Electronics, Kharkiv, Ukraine, in 1994 and 1997, respectively. He is currently a Professor with the Department of Signal Processing and Acoustics, Aalto University, Espoo, Finland. He was with the University of Alberta, Alberta, Canada, as an Assistant, an Associate, and then a Full Professor. Since his graduation, he also held various research and Faculty positions with the Kharkiv National University of Radio Electronics, the Institute of Physical and Chemical Research, Japan, McMaster University, Hamilton, Canada, Duisburg-Essen University, Duisburg, Germany and the Darmstadt University of Technology, Darmstadt, Germany, and the Joint Research Institute between Heriot-Watt University, Edinburgh EH, U.K. and Edinburgh University, Edinburgh, EH, U.K. His research interests include optimization and multiliner algebra methods in signal processing and data analysis; statistical and array signal processing; sparse signal processing; estimation, detection and learning theory and methods; and multi-antenna, very large, cooperative, and cognitive systems.

Dr. Vorobyov was the recipient of the 2004 IEEE Signal Processing Society Best Paper Award, 2007 Alberta Ingenuity New Faculty Award, the 2011 Carl Zeiss Award (Germany), 2012 NSERC Discovery Accelerator Award, and other awards. Since 2016, he has been the Senior Area Editor of the IEEE SIGNAL PROCESSING LETTERS. He was an Associate Editor for the IEEE TRANSACTIONS ON SIGNAL PROCESSING during 2006–2010 and the IEEE SIGNAL PROCESSING LETTERS during 2007–2009. He was a member of the Sensor Array and MultiChannel Signal Processing and Signal Processing for Communications and Networking Technical Committees of the IEEE Signal Processing Society during 2007–2012 and during 2010–2016, respectively. He was the Track Chair of Asilomar 2011, Pacific Grove, CA, USA, the Technical Co-Chair of the IEEE CAMSAP 2011, Puerto Rico, the Tutorial Chair of the ISWCS 2013, Ilmenau, Germany, the Technical Co-Chair of the IEEE SAM 2018, Sheffield, U.K. He is also the Technical Co-Chair of IEEE CAMSAP 2023, Costa-Rica and the General Co-Chair of EUSIPCO 2023, Helsinki, Finland.